

Optimization of bilateral filter parameters using a whale optimization algorithm

Mehrdad Nabahat, Farzin Modarres Khiyabani & Nima Jafari Navmipour |

To cite this article: Mehrdad Nabahat, Farzin Modarres Khiyabani & Nima Jafari Navmipour | (2022) Optimization of bilateral filter parameters using a whale optimization algorithm, Research in Mathematics, 9:1, 2140863, DOI: [10.1080/27684830.2022.2140863](https://doi.org/10.1080/27684830.2022.2140863)

To link to this article: <https://doi.org/10.1080/27684830.2022.2140863>



© 2022 The Author(s). This open access article is distributed under a Creative Commons Attribution (CC-BY) 4.0 license.



Published online: 23 Nov 2022.



Submit your article to this journal



Article views: 368



View related articles



View Crossmark data

Optimization of bilateral filter parameters using a whale optimization algorithm

Mehrdad Nabahat^a, Farzin Modarres Khiyabani^{ID a} and Nima Jafari Navmipour^b

^aDepartment of Mathematics, Tabriz Branch, Islamic Azad University, Tabriz, Iran; ^bDepartment of Computer Engineering, Tabriz Branch, Islamic Azad University, Tabriz, Iran

ABSTRACT

Noise removal and restoration are important topics in image processing. The filter-based denoising techniques can effectively reduce the image noise but sometimes lose image quality and information, such as blurring the edges of the image. In this paper, at first, a denoising filter is proposed by combining the whale optimization algorithm (WOA) and bilateral filter. Then, a WOA-based Richardson-Lucy (R-L) algorithm is applied to restore the image. The bilateral filter performance is largely dependent on the proper parameter selection. The bilateral filter parameters are optimized by using the weighted sum of the peak signal-to-noise ratio (PSNR) and the structural similarity index measure (SSIM) as a fitness function of the WOA algorithm to design the proposed filter. For the restoration purpose, the point spread function (PSF) of the Richardson-Lucy (R-L) algorithm is optimized by using the weighted sum of the PSNR and the second derivative like measure enhancement (SDME) as a fitness function of the WOA. The performance of the proposed denoising technique is compared with classical image denoising filters, PSO-based bilateral filters on various images and the performance of the suggested restoration technique are also compared with the blind deconvolution technique (BD) and PSO-based restoration method (BDPSO) on denoised images, with the experimental findings demonstrating that the suggested method outperforms the others. The proposed technique in the current paper can be implemented in different image applications such as medical and satellite images, etc.

ARTICLE HISTORY

Received 14 July 2020
Accepted 24 October 2022

KEY WORDS

Image denoising; image restoration; whale optimization algorithm; particle swarm optimization; bilateral filter; Richardson-Lucy algorithm; blind deconvolution technique

1. Introduction

In recent years, digital images have had many applications in different analysis and engineering sciences such as medical imaging, resonance imaging, computed tomography, satellite observation, etc. But, the image taken by sensors is usually corrupted by noise (Cho et al., 2012). Various types of noises caused by hardware or atmospheric factors such as sensor noise, camera miss focus, relative object-camera motion, and random atmospheric turbulence affect the image quality (Zhang et al., 2013). Denoising is applied to increase the quality of images as its main goal is reducing noise from the image (Sankaran et al., 2014).

There are two approaches, software-based and hardware-based denoising. While optics and hardware have been advanced to reduce undesirable effects, software-based denoising approaches, including some parameter-based denoising algorithms, because of being device-independent and widely applicable, have been highly considered.

Denoising techniques include transform-based methods, Non-local methods, and Filter-based methods.

Transform-based methods contain some linear transformations. A non-linear or multivariate operation can be done on the transformed coefficients, and an inverse of the linear transformation is applied to degenerate them into the image domain. Wavelet, curve-let, and wave atom (Hassani et al., 2010) are the transforms used for noise removal. Non-local methods estimate the intensity of all pixels based on the information about the whole image and thus use similar patterns and features in an image. In the filter-based methods, the corrupted pixels are first detected, then these pixels are modified.

Furthermore, images after being denoised seem to be blur, so image restoration is used (Gulat & Kaushik, 2012; Lv et al., 2013) to decrease the blurring of the images. The image restoration goal is to obtain the desired image from the degraded image, so it is an inverse problem. Often, the degradation process is not reversible, making image restoration problems ill-posed (Y. Zhang et al., 2012). Image restoration increases the noise, so the image denoising was done before restoration. The existing restoration techniques have been based on modeling the degradation and

CONTACT Farzin Modarres khiyabani  f.modarres@iaut.ac.ir  Associate Professor, Department of Mathematics, Tabriz Branch, Islamic Azad University, Tabriz, Iran

Reviewing editor: Yilun Shang CIS, Northumbria University, United Kingdom

© 2022 The Author(s). This open access article is distributed under a Creative Commons Attribution (CC-BY) 4.0 license.

You are free to: Share — copy and redistribute the material in any medium or format. Adapt — remix, transform, and build upon the material for any purpose, even commercially. The licensor cannot revoke these freedoms as long as you follow the license terms. **Under the following terms:** Attribution — You must give appropriate credit, provide a link to the license, and indicate if changes were made. You may do so in any reasonable manner, but not in any way that suggests the licensor endorses you or your use. **No additional restrictions** You may not apply legal terms or technological measures that legally restrict others from doing anything the license permits.

utilizing the inverse process for retrieving the original image (Conte et al., 2013; Satpathy et al., 2010). Wiener filtering (Wiener, 1975) is one of the linear processes that can be done for image restoration.

Reviewing recent studies on image denoising and restoration revealed the drawbacks of various methods and techniques applied in this field. Therefore, a new image denoising and restoration method using the metaheuristic algorithms has been proposed. In most meta-heuristic-based image restoration and noise reduction methods, only one criterion is used to evaluate the output image quality, which does not significantly improve other image quality criteria. Therefore, in this article, two important criteria are considered for image denoising, such as PSNR¹ and SSIM,² and two are used for image restoration, such as PSNR and SDME.³ Most meta-heuristic algorithms applied to Bilateral filters optimize the intensity and spatial domain parameters and assume the neighborhood radius to be constant, or Wang et al. (C. Wang et al., 2017) methods, which claim that the spatial domain parameter has little effect on the filter performance; therefore, It is assumed to be constant and optimizes the neighborhood radius and intensity domain parameter. In this paper, it is claimed that the neighborhood radius, as well as the spatial and the intensity domain parameters, significantly affect the bilateral filter's performance. Here the WOA algorithm was applied to solve the NP⁴ problem, which resulted from the anonymity of the exact values of parameters and PSF that must be optimized in the bilateral filter and the R-L algorithm, respectively. The bilateral filter parameters such as intensity domain, spatial domain, and the spatial neighborhood radius were optimized using a whale optimization algorithm. The noise-free image was achieved and compared with classical noise removal filters such as average, Gaussian, median, and PSO⁵-based bilateral filters in (C. Wang et al., 2017) and (Asokan & Anitha, 2020), respectively. The noise-free image seemed to have a few blurring effects, so the noiseless image was restored. The PSF⁶ of the R-L algorithm was optimized via the WOA algorithm and compared with the blind deconvolution technique (BD) and Kumar et al. (Kumar et al., 2017) PSO-based restoration method.

The remainder of the paper has been organized as follows: Section 2 presents a brief discussion about related noise removal and restoration research. In section 3, the bilateral filter and basic theory of WOA have been described. In Section 4, the proposed methodology and evaluation functions have been discussed. In Section 5, results and discussion have been made. Finally, the paper has ended with a conclusion in Section 6.

2. Related studies

By far, there have been several methods proposed for image denoising and restoration. This section reveals the recent studies conducted on image restoration and denoising techniques.

Image denoising's main goal is to remove the noise effectively and preserve the original image details as much as possible, and to this end, many approaches have been considered (Karnati et al., 2009).

Karnati et al. (Karnati et al., 2009) performed a denoising method to eliminate the noise successfully while maintaining the details of the original image to a feasible extent. Fathi and Naghsh-Nilchi (Fathi & Naghsh-Nilchi, 2012) proposed an efficient denoising method based on an adaptive WP⁷ thresholding function. Their adaptive technique was according to Gaussian distribution. Lee et al. (Lee et al., 2012) proposed a denoising algorithm and showed that a non-local minimum mean square error algorithm had better performance than the conventional non-local means filter (Sakthidasan & Nagappan, 2016). Wang et al. (X.-Y. Wang et al., 2013) reformed the BLS-GSM⁸ and used the SVM⁹ in the non-sub-sampled contour-let transform domain (Sakthidasan & Nagappan, 2016). Rajwade et al. (Rajwade et al., 2013) proposed an image denoising method that was simple and a patch-based machine learning technique using the HOSVD.¹⁰ Frosio and Kautz (Frosio & Kautz, 2018) presented statistical nearest neighbors for image denoising. Applying the NN¹¹ can reduce the computational burden of the Non-Local-Means algorithm. They proposed SNN¹² as an unlike neighbors' collection criterion to lighten the bias formed in the denoised patch. Their approach outperformed the traditional one in both white and colored noise. In their study, it was shown that SNN led to image quality improvement also in the case of bilateral filtering. Pan et al. (Pan et al., 2019) suggested a regularization parameter selection model for total variation in image noise removal. Firstly, for estimating an optimal upper bound, they presented an iterative algorithm by applying the consistency between the value of the data-fitting term and the upper bound. Secondly, to solve the constrained problem, they suggested a dual-based method that can skip the computation of the Lagrangian multiplier related to the constraint. The algorithm suggested by them can solve the solution of the constrained problem and simultaneously estimate the regularization parameter.

Existing noise removal methods include filter-based, non-local, and transform-based methods. Filter-based methods are divided into two categories linear and non-

linear (Chen et al., 2012). Yang et al. (Yang et al., 2010) proposed a non-local means filter to denoise the noisy images, enhance the feature recovery and particle detection, and construct a particle feature probability image according to Haar-like feature extraction. Lin (Lin, 2011) proposed a decision-based fuzzy averaging filter for noise detection and elimination that can effectively remove the impulsive noise and combine Gaussian and impulsive noise (Sakthidasan & Nagappan, 2016).

Zhang and Li (Zhang & Li, 2014) proposed a new AWMF¹³ for identifying and eliminating a high level of salt-and-pepper noise. Roy et al. (Roy et al., 2016) proposed a noise removal method utilizing an SVM classification-based FF¹⁴ for impulse noise removal in grayscale images. Wang et al. (Y. Wang et al., 2016) proposed two stages of adaptive fuzzy switching weighted mean filter to eliminate the salt and pepper noise. In the first stage, they used an improved maximum absolute luminance difference to classify pixels into three categories: uncorrupted pixels, lightly corrupted pixels, and heavily corrupted pixels. In the second stage, they used a distance-relevant adaptive fuzzy switching weighted mean filter for each pixel type to eliminate the noise. An iterative speckle filtering algorithm based on the Bayesian non-local means filter model was used by Zhou et al. (Zhou et al., 2019) for ultrasound images. The statistical feature of speckle-noise was considered for applying the BNLMF¹⁵ model to restore images, obtaining the key probability density function, and presenting an iterative filtering algorithm. They incessantly updated neighbor patches and probability density functions to achieve the filtering result closer to the potential clean one. A healthy iteration process achieved the favorable restored image, which was better than the results obtained by some typical de-speckling methods. Additionally, they declared that the benefit of the block-wise filtering style, pre-patch-selection operation, and a small iteration number, the whole algorithm is not time-consuming. Goyal et al. (Goyal et al., 2020) were reviewed a hierarchical sequence of development and creation of various Gaussian noise removal methods from the basic methods to more sophisticated hybrid techniques.

In recent years, the use of meta-heuristic algorithms that play an important role in replacing human inspections and interpreting processed images has received much attention. Khalaf et al. (Khalaf et al., 2020) used the potential of the PSO algorithm to estimate the construction costs and the duration of construction projects. Hatami et al. (Varzaneh et al., 2018) have studied the works to produce high-speed and quality association laws.

They first introduce the APRIORI-based algorithm and then use the MOPSO-ARM¹⁶ to find quality laws. Vaezinejad et al. (VaeziNejad et al., 2019) used a new intelligent hybrid method for inverse modeling (parameter identification) of leakage in the Baft Kerman dam as a case study. Their main purpose is to determine the permeability of different parts of dams using observation data. They have defined a target function that simultaneously uses the time series of hydraulic heads and flow rate observations to overcome the problem of being bad. A finite element model is developed that considers all stages of construction of an earth dam. Then, orthogonal design, artificial post-diffusion neural network, and PSO algorithm are used simultaneously to perform reverse modeling. Detecting intrusions and attacks through unauthorized users is one of the biggest challenges between cloud service providers and cloud users. So, Saljoughi et al. (Saljoughi et al., 2017) use artificial intelligence techniques such as MLP Neural Networks and PSO algorithms to detect intrusion and attacks. One of the structure's costs is the pile foundation, which can be reduced by studying the pile types and deciding on choosing the optimal pile type in terms of production cost, time, and quality. Therefore, Lateef et al. (Lateef & Burhan, 2019) have developed a model to solve the problem of finding the optimal structural pile type by using the PSO algorithm while reducing the cost and production time and increasing the quality.

Sakthidasan and Nagappan (Sakthidasan & Nagappan, 2016) combined an AGA¹⁷ and bilateral filtering to provide a noise reduction and image restoration filter. The results obtained from this technique indicated that it offered better performance in denoising all types of noisy images with a higher denoising PSNR ratio, and it restored all images with high quality. Wang et al. (C. Wang et al., 2017) proposed an automatic PSO-based (Eberhart & Kennedy, 1995) method for parameter selection of the bilateral filter (Tomasi & Manduchi, 1998) in the image denoising. The SSIM (Z. Wang et al., 2004; structural similarity index) is used as a fitness function to optimize the intensity domain and radius parameters by applying the PSO algorithm. They declared that the method they used for parameter selection was better than the other filtering methods used for denoising standard test images containing various kinds and levels of noise. Tomasi and Manduchi (Asokan & Anitha, 2020) also optimized the parameters of the bilateral filter (Tomasi & Manduchi, 1998) using PSO, cuckoo search (Yang & Deb, 2009), and adaptive cuckoo search algorithms to

reduce the satellite images that have been affected by Gaussian noise. The proposed adaptive cuckoo search method and traditional filters were compared by evaluating the PSNR, MSE, FSIM Entropy, and CPU time. It seems that their method is an edge-preserving filter and has low complexity, and is faster than other optimization algorithms. Fu et al. (Fu et al., 2014) introduced a new approach that included PSO and wiener Filter that automatically made the parameter fit for Wiener Filter in Ship Imaging System. In this method, the optimal solution was found by transferring information between individuals and information sharing, which has been a very useful parallel search algorithm with accurate parameter selection, successfully decreasing the ringing effect after image restoration and improving the image quality of restoration. Karami and Tafakori (Karami & Tafakori, 2017) proposed an image denoising method using the generalized Cauchy filter. They made a filter from GC¹⁸ distribution to remove the noise. The particle swarm optimization was used to optimize the GC filter parameters. Dou et al. (Dou et al., 2017) suggested an efficient image denoising approach based on mathematical morphology and MOPSO.¹⁹ In their approach, first, a series and parallel compound morphology filter were generated based on an open-close operation, and a structural element with various sizes aiming to remove all noises in a series link was chosen; after that, MOPSO was combined to solve the parameters' setting of multiple structural elements. Kumar et al. (Kumar et al., 2017) have proposed a method for noise removal by using a fuzzy-based median filter and then restoring the denoised image with high quality by an APSO²⁰ based Richardson-Lucy algorithm. Ye (Ye, 2013), considering the improved particle swarm optimization, represented an image restoration algorithm. His algorithm could search fast, and could effectively avoid the local optimal solution. Dash and Majhi (Dash & Majhi, 2014), proposed an image restoration method by estimating the motion-blur parameters. Their main goal was to optimize the length (L) and the blur angle (θ) of the degraded image as much as possible to improve restoration performance. Mamta and Dutta (Mamta & Dutta, 2018) have proposed a blind deconvolution technique based on the PSO and cepstrum method. A new motion blur PSF estimation method based on a criteria-cepstrum has been proposed, and then the parameters of the cepstrum were optimized through the PSO technique.

Zhang et al. (Zhang et al., 2014) proposed a Hyperspectral restoration method using low-rank matrix recovery, which could concurrently eliminate the Gaussian noise, impulse noise, deadlines, and

stripes. Bilal et al. (Bilal et al., 2016) proposed an improved PSO for image restoration. An approximated (constrained least square error) and a true cost (mean squared error) measure was used for analysis in their proposed method. An initial swarm of the heuristic solution was arbitrarily established along with problem-specific knowledge. They concluded that their method conducted better restoration than the Richardson-Lucy algorithm (Fish et al., 1995) and a state-of-the-art restoration method. Tirer and Giryes (Tirer & Giryes, 2018) proposed image restoration by iterative denoising and backward projections. To solve inverse problems, they provided a substitute method by using off-the-shelf de nosier, in which less parameter tuning is needed. In their method, firstly, a typical cost function made of fidelity and prior terms was changed into a closely relevant and new optimization problem. Then, an effective minimization scheme including a plug-and-play property was suggested, i.e. the previous term was handled just through applying a denoising operation. Lastly, an automatic tuning mechanism was provided to set the parameters used in the method. A theoretical analysis of the method was given, and its competitiveness with task-specific techniques and the P&P approach for image in painting and de blurring was empirically indicated.

Based on the results of studies, wavelets are superior because of their sparsity and multiresolution structure, and consequently, analysts have presented numerous wavelet-based algorithms for image denoising. Also, regarding the denoising issue, the fundamental denoising algorithms, specifically spatial denoising strategies and change denoising strategies, have appeared to be sufficient. However, they don't have a good performance in a few ranges which might be moved forward.

Spatial filters include some drawbacks; for instance, these filters smooth the data while decreasing noise and blurring edges in the image. Also, linear filters cannot effectively remove signal-dependent noise. Likewise, spatial frequency filtering and wavelet-based algorithms have some defects, including the calculation complexity and time-consuming. By removing these disadvantages, image denoising and consistency efficiency can be enhanced.

Filter-based denoising techniques can effectively reduce the noise, but they cannot preserve the image quality and useful information; so metaheuristic algorithms which play an important role in replacing human inspections and interpretation of processed images, have been used. The WOA algorithm is used to optimize the parameters due to two separate steps of exploration and exploitation in

almost half of the iterations that prevent the possibility of getting stuck in local optima and having a high convergence speed. Therefore, the current paper aimed to denoise images through the WOA algorithm in a bilateral filter to optimize the filter parameters and restore the images using the WOA in the Richardson-Lucy algorithm.

The advantages of the proposed method include simple design, significant noise removal and restoration, and preservation of image information. Still, in the proposed methods, the original noiseless image must be accessible for comparison. When the weighted sum of the two objective functions is used as a fitness function, some optimal solutions may be omitted, which are the disadvantages of the proposed method.

3. Noise removal

In this section, a filter-based technique, namely a bilateral filter, was used for noise removal. The filter parameters were optimized using the WOA algorithm, which has been described.

3.1 Bilateral filter

The Bilateral filter proposed by Tomasi (Tomasi & Manduchi, 1998) has been a non-linear, edge-preserving, and noise-reducing smoothing filter for images, in which the intensity of each pixel was substituted with a weighted average of intensity values from nearby pixels. The Gaussian distribution could be considered as the base for this weight. The weights were influenced by the Euclidean distance of pixels and the radiometric differences that kept edges safe. The output of the bilateral filter for the pixel located in (x, y) was calculated as follows:

$$I^f(x, y) = \frac{1}{W} \sum_{(i,j) \in \Omega(x,y)} I(x, y) e^{-\frac{\|(x,y)-(i,j)\|^2}{2\sigma_d^2}} \times e^{-\frac{|I(x,y)-I(i,j)|^2}{2\sigma_r^2}} \quad (1)$$

and normalization term, W , is defined as:

$$W = \sum_{(i,j) \in \Omega(x,y)} e^{-\frac{\|(x,y)-(i,j)\|^2}{2\sigma_d^2}} \times e^{-\frac{|I(x,y)-I(i,j)|^2}{2\sigma_r^2}} \quad (2)$$

Where $I(x, y)$, $I^f(x, y)$ represent the pixel intensity and filtered pixel intensity at the location of (x, y) , and σ_d, σ_r are parameters controlling the fall-off of loads in the spatial and intensity domains; respectively. $\Omega(x, y)$ was a spatial neighborhood of (x, y) . The performance of the bilateral filter depended on the proper

selection of three parameters σ_d, σ_r, d ; d is considered a radius of $\Omega(x, y)$. However, selecting appropriate parameter values was frequently required according to the user's previous experience.

3.2 Whale optimization algorithm (WOA)

The whale optimization algorithm has been a newly presented nature-stimulated algorithm suggested by Mirjalili and Lewis (Mirjalili & Lewis, 2016), which imitates the hunting activities of humpback whales. One of the hunting behaviors of whales is that they dive about 12 meters under the prey and begin to form bubbles in a twisting form around the prey, then come to the water surface to catch the prey. The mathematical modeling of the WOA algorithm has been clarified as follows. For more information, refer to (Mirjalili & Lewis, 2016).

3.2.1 Surrounding prey

Humpback whales can detect the position of the prey and can surround it. Since the exact location of the prey (optimal solution) is unknown, the whale algorithm considers the best current solution as the target or close to the target, and other whales update their position according to the current solution. This act has been exemplified as follows in Eq. (3) and (4).

$$\vec{R} = \left| \vec{W} \cdot \vec{L}^*(t) - \vec{L}(t) \right| \quad (3)$$

$$\vec{L}^*(t+1) = \vec{L}^*(t) - \vec{V} \cdot \vec{R} \quad (4)$$

where "t", \vec{L}^* and \vec{L} signify the current iteration, the current finest solution, and the location vector respectively, " $| |$ " is the absolute value, " \cdot " is elementwise multiplication. If there is a superior solution, \vec{L}^* it should be updated. The vectors \vec{V}, \vec{W} have been figured as follows:

$$\vec{V} = 2\vec{m} \cdot \vec{n} - \vec{m} \quad (5)$$

$$\vec{W} = 2\vec{n} \quad (6)$$

The exploration and exploitation phases are reduced from 2 to 0 through the iterations and \vec{n} is a random value in $[0, 1]$.

3.2.2 Bubble-net attacking method (exploitation phase)

The bubble-net attacking of humpback whales contains two methods; the first approach is the shrinking surrounding technique which is accomplished by reducing

the value of \overrightarrow{m} in Eq. (5); correspondingly, the amount of \overrightarrow{V} is also decreased. The second approach is the spiral updating position technique in which whales try to imitate the helix-shaped movement around the best solution (prey) as follows:

$$\overrightarrow{L}(t+1) = \overrightarrow{R} \cdot e^{cf} \cdot \cos(2\pi f) + \overrightarrow{L}^*(t) \quad (7)$$

The distance between the prey and i^{th} whale is designated by, c and f are constant and arbitrary numbers in $[-1, 1]$, respectively. The humpback whales swim around the prey within a shrinking circle and along a spiral-shaped route simultaneously. Therefore, this conduct has been modeled by giving the identical likelihood of happening to both of the methods as follows:

$$\overrightarrow{L}(t+1) = \begin{cases} \overrightarrow{L}^*(t) - \overrightarrow{V} \cdot R p < 0.5 \\ \overrightarrow{R} \cdot e^{cf} \cdot \cos(2\pi f) + \overrightarrow{L}^*(t) p \geq 0.5 \end{cases} \quad (8)$$

where p is a random number in $[0, 1]$.

3.2.3 Search for prey (exploration phase)

Changes in \overrightarrow{V} values are considered as the exploration phase. In this phase, the humpback whales search arbitrarily according to the location of each one. The arbitrary values for \overrightarrow{V} is greater than -1 or less than 1 to force the whale to travel far away from the reference whale. In the exploration phase, the position of the whales is updated according to the randomly selected whale. The mechanism and $|\overrightarrow{V}|$ highlighted the exploration and made it possible for the WOA algorithm

to conduct a global search. The mathematical model was as follows:

$$\overrightarrow{R} = |\overrightarrow{W} \cdot \overrightarrow{L}_{rand}(t) - \overrightarrow{L}(t)| \quad (9)$$

$$\overrightarrow{L}(t+1) = \overrightarrow{L}_{rand}(t) - \overrightarrow{V} \cdot \overrightarrow{R} \quad (10)$$

$\overrightarrow{L}_{rand}$ is an arbitrarily selected whale in a group of existing whales. The WOA algorithm starts to find the best solution by arbitrarily tracing the whales in the search space. In each repetition, the whales update their location according to either the finest whale or arbitrarily selected whale. The value p reveals that the whales should have a spiral or circular movement. The WOA algorithm ends when a predetermined termination condition is met.

4. Proposed denoising and restoration method

This paper proposed a filter that used the bilateral filter and the WOA algorithm for noise removal of the images affected by Gaussian and salt and pepper (SAP) noise. Then, the PSF of the R-L²¹ algorithm was optimized for restoration purposes. Assume that I will be a $M \times N$ noisy image. At first, the noise-free image was obtained through the denoising step, and then the noiseless image was restored by R-L. Image denoising and restoration can be achieved through optimizing the bilateral filter parameters and the PSF of the R-L algorithm, respectively. The proposed method for noise removal was compared with classical

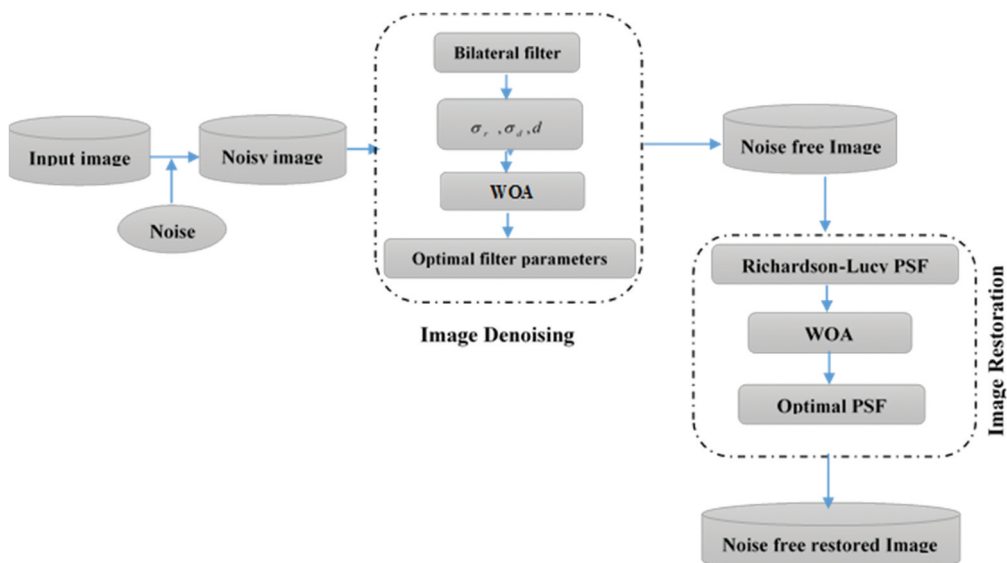


Figure 1. The diagram of the proposed method.

filters like the average filter, Gaussian filter, median filter, the PSO-based bilateral filter of Wang et al. (C. Wang et al., 2017), and the PSO-based bilateral filter used in (Asokan & Anitha, 2020), the proposed technique for image restoration was compared with the BD technique and PSO based (BDPSO) described in (Kumar et al., 2017). The diagram of the proposed method is illustrated in Figure 1.

4.1 Image denoising using the WOA algorithm for bilateral filter

A filter that optimized the bilateral filter parameters was designed for noise removal. Here, the images corrupted by Gaussian or SAP noise were denoised with a bilateral filter. After noise removal, the images were sent to the restoration process. The restoration process was done on noiseless images by optimizing the PSF of the R-L algorithm by applying the WOA. Proper parameter selection is needed to improve the performance of the bilateral filter in noise removal. While there is no suitable technique for optimal parameter selection, the WOA algorithm was used for optimizing the bilateral filter parameters. The parameters of the spatial domain σ_d and the intensity domain σ_r of the bilateral filter were optimized by using different meta-heuristic algorithms such as AGA (Sakthidasan & Nagappan, 2016), PSO (C. Wang et al., 2017), and cuckoo search algorithm (Asokan & Anitha, 2020) by considering the PSNR or MSE, or SSIM as a fitness function. In all methods, only one criterion is used to evaluate the quality of the denoised image. The spatial neighborhood radius in all methods except the Wang et al. (C. Wang et al., 2017) method is considered constant. Wang et al. (C. Wang et al., 2017) proposed that the spatial domain parameter of the bilateral filter does not have much effect on the filter performance. Still, the filter performance depended on the spatial neighborhood radius d , so choosing an appropriate radius d was needed. Experimental results on different images showed that the spatial domain parameter and the neighborhood radius significantly affect the filter performance and should be optimized. Therefore the spatial domain σ_d , the intensity domain σ_r , and radius parameter d are optimized.

Since, in most papers, only one criterion is used to evaluate the image quality in meta-heuristic algorithms, a multi-objective problem has been considered here. The objectives were the PSNR and the SSIM, which should be maximized. The PSNR (Moreno et al., 2013), which could describe the noiseless image quality, was as follows:

$$F_1 = PSNR = 10 \log_{10} \frac{MAX^2}{MSE} \quad (11)$$

$$MSE = \frac{1}{M \times N} \sum_{i=1}^M \sum_{j=1}^N (I(x, y) - I_n(x, y))^2 \quad (12)$$

Where MSE is the mean squared error, MAX is the maximum intensity value of pixels, usually 255, I and I_n are original and noisy images, respectively.

The SSIM (Z. Wang et al., 2004) measured the similarity between two images. The SSIM is described as follows:

$$F_2 = SSIM = \frac{(2\mu_I\mu_{I_n} + c_1)(2\sigma_{I,I_n} + c_2)}{(\mu_I^2 + \mu_{I_n}^2 + c_1)(\sigma_I^2 + \sigma_{I_n}^2 + c_2)} \quad (13)$$

Where, μ_I, μ_{I_n} and $\sigma_I^2, \sigma_{I_n}^2$ are the mean value and variance value of corresponding original and noisy images, and σ_{I,I_n} is the covariance between original and noisy image. $c_1 = (0.01 \times 255)^2, c_2 = (0.03 \times 255)^2$ are two constants. The weighted sum method was used to solve the multi-objective problem, so the fitness function has been defined as follows:

$$fitness = w_1 F_1 + w_2 F_2 \quad (14)$$

Where, $w_1, w_2 \geq 0$ weight, and $w_1 + w_2 = 1$. In this paper w_1, w_2 were considered 0.5.

Initially, the total number of n search agents was generated, each containing bilateral filter parameters. Then, these parameters in each search agent were optimized using the fitness function Eq. (14), and the best answer was provided. The process of the WOA was iterated T times until the maximum value of the fitness function was gained. Finally, a noise-free image was obtained using the best parameters for the bilateral filter. The pseudo-code of the proposed denoising filter is exemplified as follows:

4.2 Image restoration using WOA

The noiseless image seemed to be blurred. The WOA algorithm was used in the R-L algorithm to improve the noiseless images. The PSF was optimized through the WOA algorithm to recover the blurred images. In this paper, 20 search agents (PSF) have been randomly generated where each PSF is a 3*3 matrix, and its elements are between 0, 1. Since in (C. Wang et al., 2017) and (Sakthidasan & Nagappan, 2016), only the SDME is used to optimize the PSF of the R-L algorithm, and increasing this criterion reduces the PSNR in some

The pseudo-code of the proposed denoising filter

```

Enter the original image.
Corrupt the original image by different levels of Gaussian and the SAP noise
Initialize search agents randomly, which each contain 3 parameters
Apply Eq (2) to all pixels of the noisy image, according to the parameters that have been initialized.
Different de-noised images are obtained.
Iter=1
Calculate the fitness function for each search agent, using Eq (14) and consider as the best
solution.
while Iter < maxiter
    for all search agents
        Update
        if
            if
                Update search agents location through Eq (3)
            else if \
                Select a search agent randomly.
                Update search agents location through Eq (10)
            end if
            elseif
                Update search agents location through Eq (7)
            end if
        end for
        If the search agent is out of the search space, return it back
        Calculate the fitness function for each search agent
        Update if there is a better solution.
        Iter=Iter+1
    end while
    return
The de-noised image is obtained with the maximum fitness function.

```

images, the fitness function of the generated search agents was considered a multi-objective problem. It contained two objectives that should have been maximized. For solving the multi-objective problem, the weighted sum method was considered.

The first considered objective function was the PSNR, and the second one was the SDME (Sakthidasan & Nagappan, 2016), which has been a measure to assess the performance of the enhanced images and was defined as follows:

$$SDME = -\frac{1}{b_1 \cdot b_2} \sum_{i=1}^{b_1} \sum_{j=1}^{b_2} 20 \ln \left| \frac{P_{max,j,i} - 2P_{cen,j,i} + P_{min,j,i}}{P_{max,j,i} + 2P_{cen,j,i} + P_{min,j,i}} \right| \quad (15)$$

Suppose that the image was divided into $b_1 \times b_2$ blocks, P_{max} , P_{min} , P_{cen} each block's maximum, minimum, and center intensity values, respectively. All of

the search agents were evaluated by the fitness function defined below:

$$fitness = w_1 PSNR + w_2 SDME \quad (16)$$

Where $w_1, w_2 \geq 0$ are weights and $w_1 + w_2 = 1$.

At each iteration, the point spread function of the R-L got better by using the fitness function. The process was repeated T times until the maximum value of the fitness function was achieved. Finally, the enhanced and restored image was obtained by optimizing the PSF of the R-L. The pseudo-code of the proposed restoration method is as follows:

4.4 Parameter setting

In the proposed noise reduction filter and the PSO-based bilateral filters, the maximum number of iterations and the population size are 50 and 20, respectively.

The pseudo-code of the proposed restoration method

```

Enter the filtered image.
Initialize search agents randomly, where each search agent is a 3*3 matrix and its elements are between 0,1.
Apply the R-L algorithm to the noiseless images according the PSFs that have been initialized.
Different restored images are obtained.
Iter=1
Calculate the fitness function for each search agent, using Eq (16) and consider as the best solution.
while Iter < maxiter
    for all search agents
        Update
        if
            if
                Update search agents location through Eq (3)
            else if
                Select a search agent randomly.
                Update search agents location through Eq (10)
            end if
        elseif
            Update search agents location through Eq (7)
        end if
    end for
    If the search agent is out of the search space, return it back
    Calculate the fitness function for each search agent
    Update if there is a better solution.
    Iter=Iter+1
end while
return
The restored image is obtained with the maximum fitness function.

```

Given the stochastic nature of the proposed methods and PSO-based filters, the presented results are an average of 30 times, the execution of these algorithms.

The WOA parameters follow the values given in Section 3.2, and the PSO parameters are considered the same as (C. Wang et al., 2017).

The spatial domain, intensity domain, and the radius parameter in the PSO-based bilateral filter (C. Wang et al., 2017) are considered as follows:

$$\sigma_d = 10, \sigma_r \in [1, 200], d \in [1, 5] \quad (17)$$

The spatial domain, intensity domain, and the radius parameter in the proposed filter are considered as follows:

$$\sigma_d = [0.1, 10], \sigma_r \in [1, 200], d \in [1, 5] \quad (18)$$

5. Results and discussion

The grayscale input image was corrupted by three standard deviations ($\sigma = 30, 50, 70$) of the Gaussian noise and three different densities ($d = 0.02, 0.03, 0.05$) of SAP noise. The noisy images were denoised using the classical filters such as the Average filter, Gaussian filter,

median filter, and two PSO-based Bilateral filters such as BPSO-W, BPSO-A, and the proposed filter (BProposed), and then the noiseless images were restored by BD, BDPSO and the proposed restoration method. The BProposed technique performance was analyzed using the fitness function in Eq. (14), which includes two measures: PSNR and SSIM. The fitness function in Eq. (16) evaluated the proposed restoration method containing two measures: PSNR and SDME. To make a fair comparison between the noise reduction filters, in all images, the PSNR and SSIM values between the filtered and the original images, except for the proposed filter, are calculated manually. The performance of the proposed filter was compared with the existing filters, such as the average filter, Gaussian filter, median filter, and PSO-based bilateral filter used in (C. Wang et al., 2017) and (Asokan & Anitha, 2020). To this end, six grayscale images such as Lena 512 × 512, Iris 300 × 300, Baboon 256 × 256, cameraman 256 × 256, Pepper 256 × 256, and Gold-Hill 256 × 256 are considered. These images are the noiseless test images in the field of image processing. Each resolution is 8 bits per pixel and corrupted by different standard deviations ($\sigma_n = 30, 50, 70$) of the Gaussian noise. Also, six

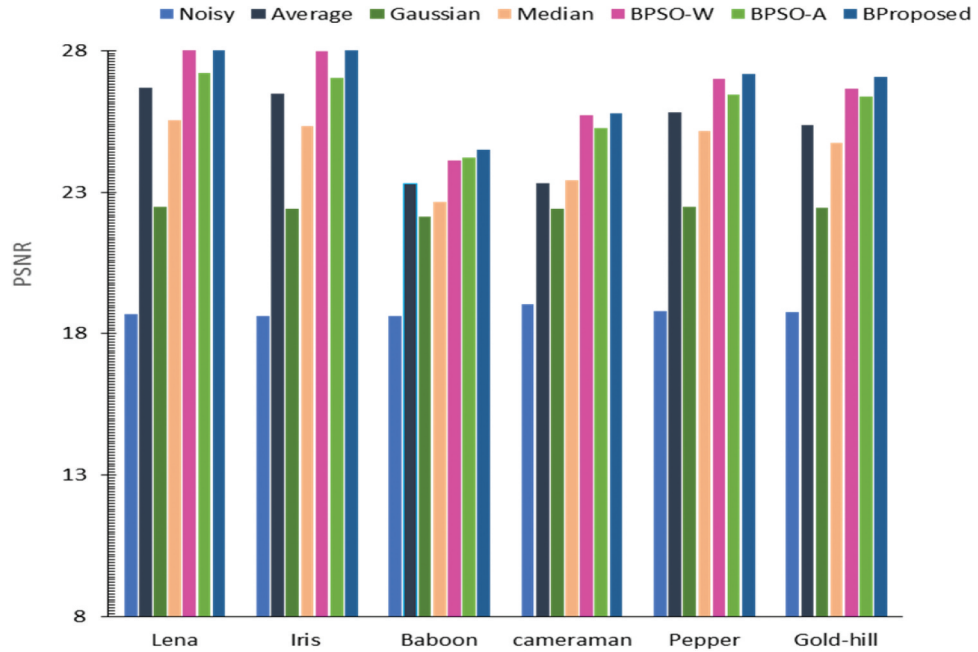


Figure 2. PSNR value of the Proposed and existing filters with Gaussian noise ($\sigma_n = 30$).

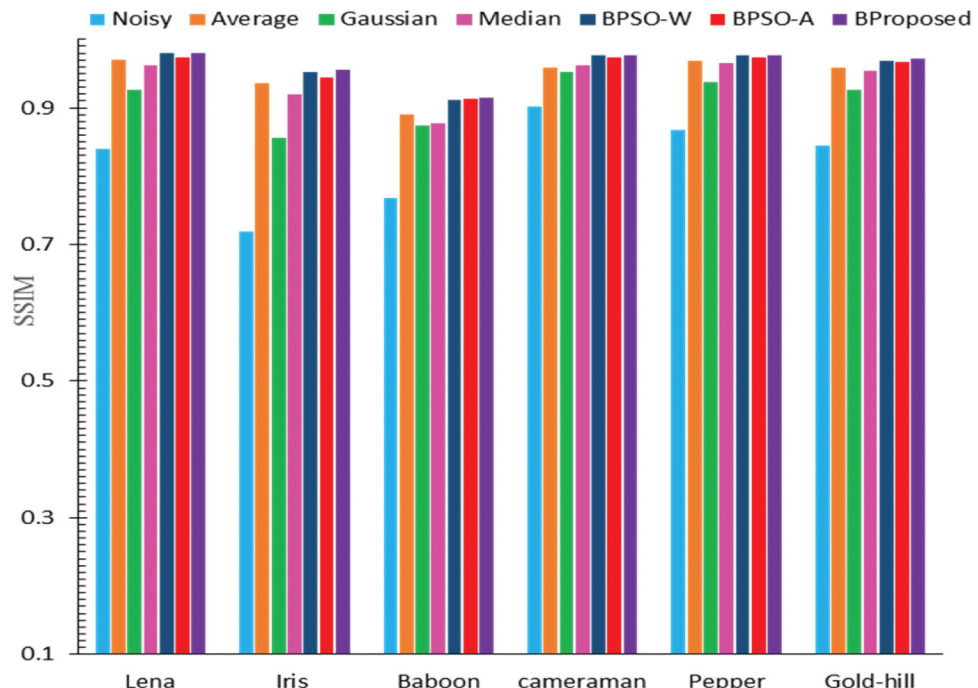


Figure 3. SSIM value of the BProposed and existing filters with Gaussian noise () .

different grayscale images such as Barbara 512×512 , Boats 512×512 , Hill 512×512 , Couple 512×512 , Peppers 256×256 , and House 256×256 were corrupted by different densities ($d = 0.02, 0.03, 0.05$) of the SAP noise. The PSNR, SSIM, and fitness values were calculated for all images that were corrupted by various Gaussian noise standard deviations, and the

outcomes are shown in Table 1. Figures 2–4 show a schematic representation of the findings. As an illustration, the results of the suggested filter's actual comparison are displayed on a few images in Figure 5. The images Baboon Lena are corrupted with various standard deviations (30, 50 and 70) of the Gaussian noise, respectively. Figure 5 a, b, c, d, e, f, g, and

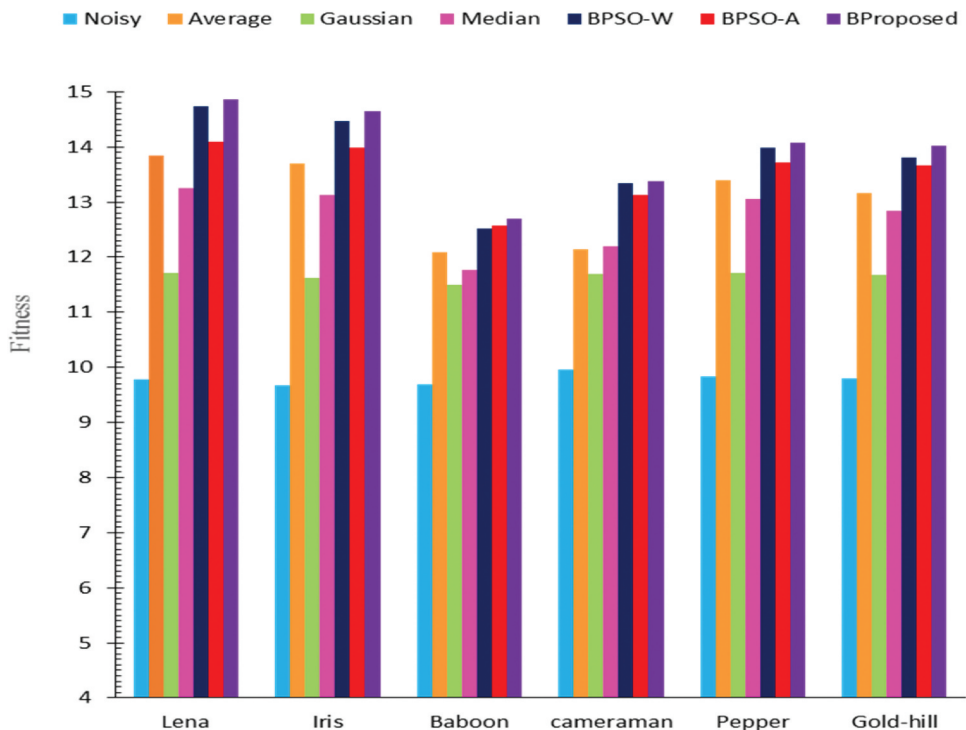


Figure 4. The fitness value of the BProposed and existing filters with Gaussian noise ($\sigma_n = 30$).

h represent the Original, Noisy, Average filter, Gaussian filter, Median filter, BPSO-W filter, BPSO-A filter, and proposed filter, respectively. A similar operation is done for images corrupted by the SAP noise, and the results are placed in Table 2. As a sample, the results obtained from the filters for SAP noise

reduction with a density of 0.05 for the Hill image are shown in Figure 6. For instance, the practical comparison results have been shown on some images in Figure 7, in which the images *HillPeppers* are corrupted with different densities ($d = 0.02, 0.03, 0.05$) of SAP noise, respectively.

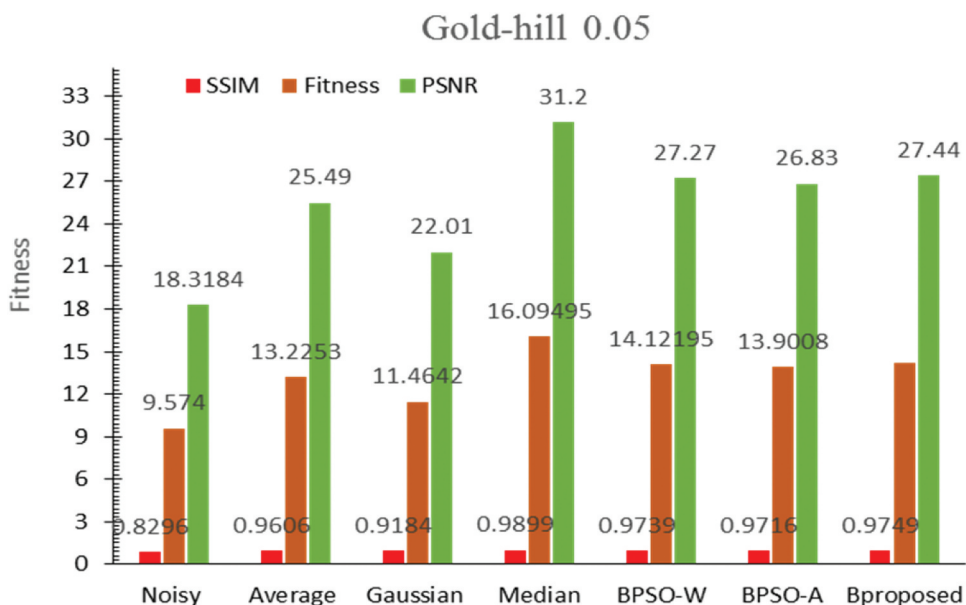


Figure 5. Images resulting from Gaussian noise reduction filters.

Table 1. Implementation of different denoising methods on several images with various Gaussian noise

σ_n		Images	Noisy	Average	Gaussian	Median	BPSO-W	BPSO-A	BProposed
30	PSNR	Lena	18.7037	26.6978	22.4804	25.5421	28.4794	27.2053	28.7281
		Iris	18.6339	26.4754	22.4035	25.3452	27.9897	27.0321	28.3528
		Baboon	18.6276	23.281	22.1182	22.6603	24.1227	24.2303	24.4799
		cameraman	19.0191	23.3091	22.4213	23.4281	25.7119	25.2719	25.7803
		Pepper	18.7873	25.8087	22.4756	25.1487	27.0026	26.4476	27.1813
	SSIM	Gold-hill	18.7441	25.3522	22.4304	24.7261	26.6459	26.3567	27.0762
		Lena	0.8402	0.9699	0.9255	0.9616	0.9796	0.9733	0.9807
		Iris	0.7181	0.9362	0.8562	0.9195	0.9522	0.9436	0.9559
		Baboon	0.7682	0.8908	0.8746	0.8778	0.9118	0.9137	0.9154
		cameraman	0.9025	0.9586	0.9519	0.9617	0.9767	0.9743	0.977
	Fitness	Pepper	0.868	0.9694	0.9381	0.9655	0.9765	0.9738	0.9775
		Gold-hill	0.8443	0.9592	0.9256	0.9544	0.9693	0.9679	0.9723
		Lena	9.77195	13.83385	11.70295	13.25185	14.7295	14.0893	14.8544
		Iris	9.676	13.7058	11.62985	13.13235	14.47095	13.98785	14.65435
		Baboon	9.6979	12.0859	11.4964	11.76905	12.51725	12.572	12.69765
50	PSNR	cameraman	9.9608	12.13385	11.6866	12.1949	13.3443	13.1231	13.37865
		Pepper	9.82765	13.3886	11.70685	13.0571	13.98955	13.7107	14.0794
		Gold-hill	9.7942	13.1557	11.678	12.84025	13.8076	13.6623	14.02425
		Lena	14.6153	23.3914	18.4127	21.5706	26.1266	23.4767	26.1558
		Iris	14.4493	23.1938	18.2501	21.4243	25.6388	23.2667	26.2003
	SSIM	Baboon	14.4564	21.38	18.1319	20.1041	22.4172	21.6485	22.8181
		cameraman	14.8704	21.2487	18.4087	20.5763	22.4964	21.8498	22.5402
		Pepper	14.7138	22.822	18.4344	21.3592	24.3447	22.9693	24.6117
		Gold-hill	14.6599	22.6022	18.3893	21.1569	24.5792	22.9905	25.0707
		Lena	0.6635	0.9354	0.824	0.9092	0.9633	0.9371	0.9635
	Fitness	Iris	0.4855	0.8698	0.6896	0.8224	0.9180	0.8728	0.9249
		Baboon	0.5521	0.8365	0.7302	0.7989	0.8619	0.8474	0.8701
		cameraman	0.7711	0.9319	0.8816	0.9273	0.9489	0.942	0.9494
		Pepper	0.7113	0.9386	0.8513	0.9206	0.9551	0.9413	0.9574
		Gold-hill	0.6691	0.9225	0.8241	0.9013	0.9490	0.9301	0.9537
70	PSNR	Lena	7.6394	12.1634	9.61835	11.2399	13.54495	12.2069	13.55965
		Iris	7.4674	12.0318	9.46985	11.12335	13.2784	12.06975	13.5626
		Baboon	7.50425	11.10825	9.43105	10.4515	11.63955	11.24795	11.8441
		cameraman	7.82075	11.0903	9.64515	10.7518	11.72265	11.3959	11.7448
		Pepper	7.71255	11.8803	9.64285	11.1399	12.6499	11.9553	12.78455
	SSIM	Gold-hill	7.6645	11.76235	9.6067	11.0291	12.7641	11.9603	13.0122
		Lena	12.226	21.0873	15.9977	18.8641	24.284	20.8317	24.4578
		Iris	12.0513	20.9871	15.8428	18.7021	24.165	20.6503	24.2559
		Baboon	12.0784	19.7955	15.7802	17.9203	21.6245	19.7188	21.8773
		cameraman	12.4355	19.4542	15.9646	18.3133	20.6989	19.656	20.9678
	Fitness	Pepper	12.3296	20.6248	16.0202	18.7362	22.4217	20.4676	22.7223
		Gold-hill	12.2677	20.4993	15.9703	18.5986	23.1392	20.4825	23.3454
		Lena	0.5137	0.8878	0.7138	0.8424	0.9418	0.8839	0.9436
		Iris	0.337	0.7905	0.5445	0.7119	0.8789	0.7811	0.8771
		Baboon	0.3998	0.7684	0.5952	0.7059	0.8223	0.7709	0.8301
	Fitness	cameraman	0.6404	0.8937	0.7971	0.8811	0.9187	0.9012	0.9223
		Pepper	0.5693	0.8955	0.7532	0.8624	0.9278	0.8944	0.9312
		Gold-hill	0.5195	0.8719	0.7135	0.8335	0.9246	0.8753	0.9277
		Lena	6.36985	10.98755	8.35575	9.85325	12.6129	10.8578	12.7007
		Iris	6.19415	10.8888	8.19365	9.707	12.52195	10.7157	12.5665
	BPSO-A	Baboon	6.2391	10.28195	8.1877	9.3131	11.2234	10.24485	11.3537
		cameraman	6.53795	10.17395	8.38085	9.5972	10.8088	10.2786	10.94505
		Pepper	6.44945	10.76015	8.3867	9.7993	11.67475	10.681	11.82675
		Gold-hill	6.3936	10.6856	8.3419	9.71605	12.0319	10.6789	12.13655

As shown in Table 1 and Figures 2–4, the proposed filter attained higher PSNR, SSIM, and fitness values than the existing noise removal methods, including classical filters and the BPSO-W (C. Wang et al., 2017), BPSO-A (Asokan & Anitha, 2020). The proposed filter outperformed the BPSO-W and BPSO-A filters in comparison to the results, while the BPSO-W and BPSO-A methods outperformed the classical filters. The reason behind it

was that in the proposed method, three parameters σ_d, σ_r, d were optimized so that two objective functions of SSIM and PSNR were maximized. At the same time, in the BPSO-W, the spatial domain of the bilateral filter is considered constant. Only the parameters (σ_r, d) of the bilateral filter were optimized for maximizing the SSIM as the objective function, or in the BPSO-A, the spatial neighborhood radius (d) considered constant. Only the parameters

**Table 2.** Implementation of different denoising methods on several images with SAP noise

SNR	Barbara	Average	Gaussian	Median	BPSO-W	BPSO-A	BProposed
SSIM	Boats	0.02 0.03 0.05	24.12 23.77 23.01	25.19 23.80 21.64	25.31 25.25 25.13	25.10 24.72 23.95	25.70 24.98 23.96
	Hill	0.02 0.03 0.05	27.05 26.38 25.20	25.92 24.34 22.13	30.79 30.67 30.39	28.38 27.70 26.37	28.39 27.70 26.60
	Couple	0.02 0.03 0.05	27.65 26.79 25.49	26.03 24.21 22.01	31.50 31.43 31.20	29.13 28.22 27.27	29.13 28.23 27.44
	Peppers	0.02 0.03 0.05	26.85 26.19 25.13	25.93 24.32 22.19	30.42 30.34 30.14	28.15 27.46 26.34	28.15 27.46 26.47
	House	0.02 0.03 0.05	25.65 25.20 24.22	25.56 24.26 21.93	31.91 31.60 30.99	27.61 26.95 25.63	27.61 26.95 25.63
	Barbara	Average	Gaussian	Median	BPSO-W	BPSO-A	BProposed
	Boats	0.02 0.03 0.05	0.9556 0.9517 0.9417	0.9667 0.9544 0.9256	0.9671 0.9666 0.9657	0.9649 0.9617 0.9540	0.9697 0.9640 0.9540
	Hill	0.02 0.03 0.05	0.9696 0.9644 0.9530	0.9622 0.9462 0.9119	0.9875 0.9872 0.9863	0.9778 0.9740 0.9646	0.9778 0.9740 0.9656
	Couple	0.02 0.03 0.05	0.9646 0.9587 0.9468	0.9585 0.9403 0.9045	0.9905 0.9904 0.9899	0.9834 0.9795 0.9739	0.9834 0.9792 0.9749
	Peppers	0.02 0.03 0.05	0.9671 0.9634 0.9536	0.9679 0.9570 0.9271	0.9926 0.9920 0.9908	0.9793 0.9759 0.9672	0.9793 0.9759 0.9672
	House	0.02 0.03 0.05	0.9696 0.9638 0.9542	0.9614 0.9429 0.9135	0.9935 0.9931 0.9928	0.9844 0.9800 0.9744	0.9844 0.9800 0.9753
Fitness	Barbara	Average	Gaussian	Median	BPSO-W	BPSO-A	BProposed
	Boats	0.02 0.03 0.05	12.5378 12.36085 11.97585	13.07835 12.3772 11.2828	13.13855 13.1083 13.04785	13.03245 12.84085 12.452	13.33485 12.972 12.457
	Hill	0.02 0.03 0.05	14.0098 13.6722 13.0765	13.4411 12.6431 11.52095	15.88875 15.8286 15.68815	14.6789 14.337 13.6673	14.68895 14.337 13.67225
	Couple	0.02 0.03 0.05	14.31325 13.88055 13.2253	13.49855 12.58005 11.4642	16.24525 16.2102 16.09495	15.0567 14.59975 14.12195	15.0567 14.6046 14.20745
	Peppers	0.02 0.03 0.05	13.9073 13.57435 13.0384	13.44425 12.63015 11.54725	15.70245 15.6623 15.56195	14.562 14.21475 13.65015	14.562 14.2147 13.71525
	House	0.02 0.03 0.05	14.0348 13.6619 13.1621	13.4407 12.55645 11.60675	16.4513 16.296 15.9904	14.29465 13.96295 13.2986	14.29465 13.96295 13.2986

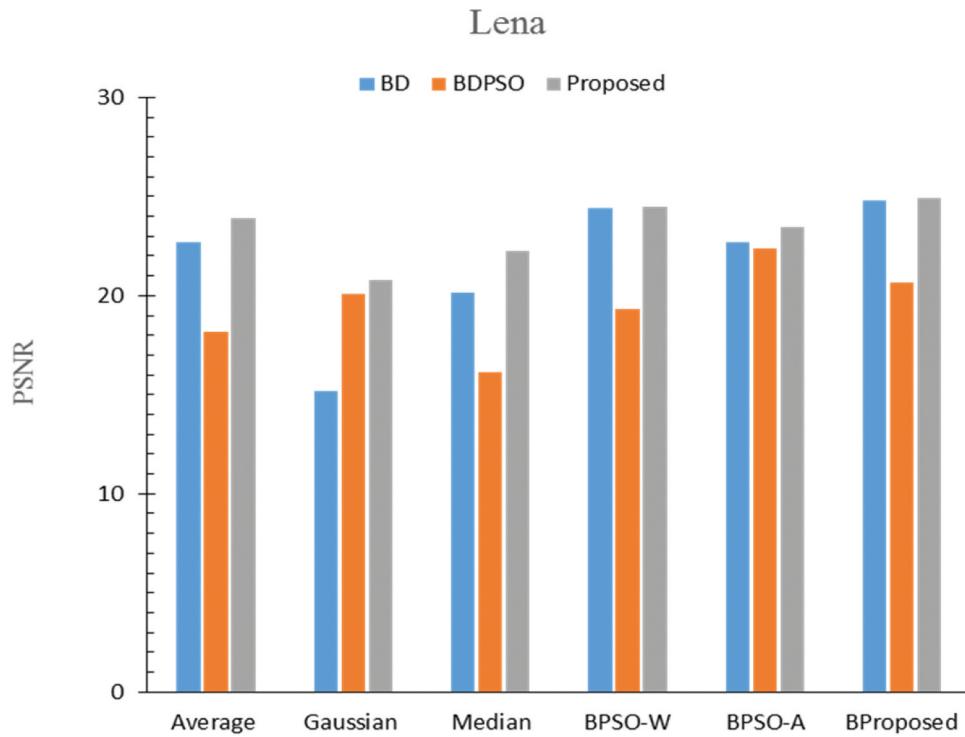


Figure 6. PSNR, SSIM, Fitness values of the BProposed, and existing filters with SAP noise.

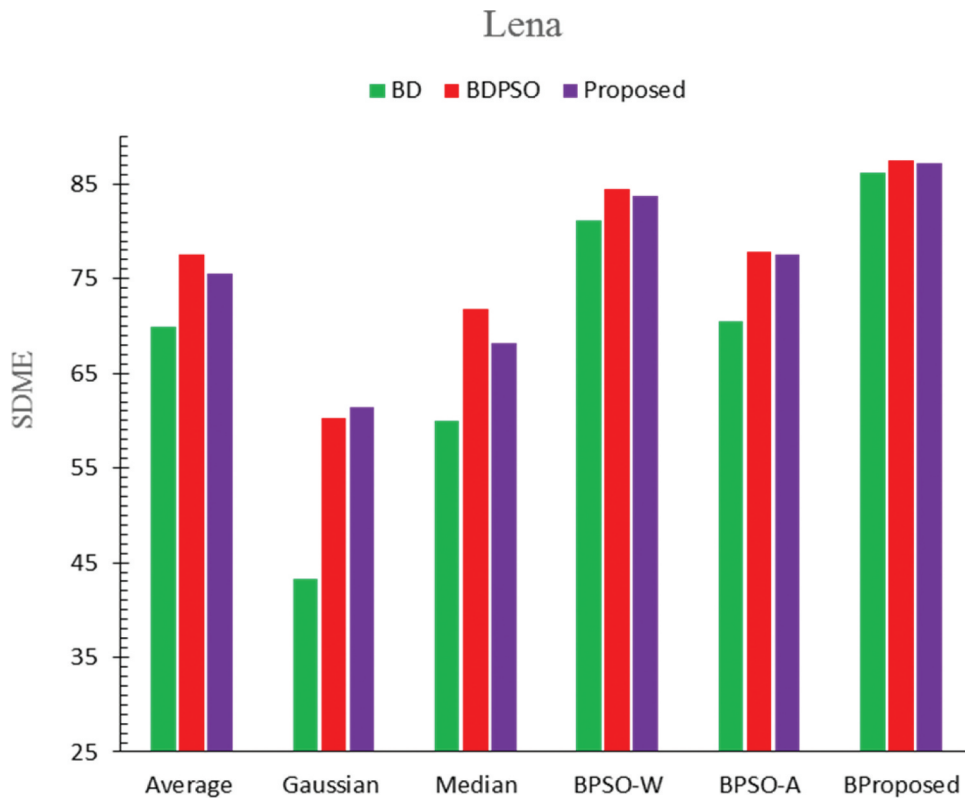


Figure 7. Images resulting from SAP noise reduction filters.

**Table 3.** Implementation of BD, BDPSo, and proposed restoration methods on denoised images

$\sigma_n = 30$	PSNR	Images	Average filter				Gaussian filter				Median filter				BPSO-W				BPSO-A				BProposed				
			BD		BDPSO		Proposed		BD		BDPSO		Proposed		BD		BDPSO		Proposed		BD		BDPSO		Proposed		
			BD	BDPSO	BD	BDPSO	Proposed	BD	BDPSO	Proposed	BD	BDPSO	Proposed	BD	BDPSO	Proposed	BD	BDPSO	Proposed	BD	BDPSO	Proposed	BD	BDPSO	Proposed		
SDME	Lena	22.6802	18.1437	23.8837	15.1571	20.1181	20.7653	20.1611	16.163	22.25	24.4507	19.3343	24.5092	22.6787	22.3735	23.4748	24.8081	20.6386	24.9153	24.2125	21.254	24.2299	19.1107	19.4411	20.2694		
	Iris	22.2518	20.8833	22.595	14.9085	19.2648	20.5906	19.9722	20.1904	21.9247	23.7879	16.128	23.8411	19.8767	22.2697	22.2697	24.2125	21.254	21.254	17.657	19.8376	19.1107	19.4411	20.2694			
	Baboon	20.6552	19.073	20.8476	14.2979	18.1985	18.6214	18.9034	15.533	19.3241	19.399	19.399	21.6662	19.5795	17.657	18.8757	19.8757	17.9878	17.9878	21.216	21.216	19.8757	19.8757	21.216			
	cameraman	19.4363	16.5917	20.4111	16.383	16.921	17.9706	18.0989	18.7224	18.8559	18.4753	18.356	18.7035	18.9675	17.6827	21.0969	21.0969	18.8757	18.8757	17.9878	17.9878	19.8757	19.8757	21.216			
	Pepper	20.8133	21.2973	21.4014	15.0093	18.307	20.1249	19.0729	18.4804	19.60	21.7167	18.7131	21.8599	21.0833	17.8375	21.5242	21.5242	21.9426	21.9426	17.4591	17.4591	19.4318	19.4318	21.4318	21.4318		
	Gold-hill	20.713	18.9677	20.7521	14.7233	17.2986	19.699	18.9094	20.4812	20.432	21.1929	19.976	21.2272	20.61	19.7288	20.8713	20.8713	21.417	21.417	19.4318	19.4318	21.4318	21.4318	21.4318	21.4318		
	Lena	69.9498	77.5398	75.4972	43.2868	60.3463	61.4075	60.0206	71.7637	68.2654	81.1573	84.4607	83.6903	70.564	77.8839	77.5875	86.1942	87.5125	87.1443	87.1443	84.2333	84.2333	83.954	84.8997	84.2333	84.2333	
	Iris	67.3427	74.8874	74.3273	41.6423	58.582	58.56	58.2319	69.0578	69.7514	77.8787	82.0748	80.891	67.913	75.9412	75.7954	86.8609	86.8609	86.8609	86.8609	86.8609	86.8609	86.8609	86.8609	86.8609	86.8609	
	Baboon	68.4574	75.533	74.9197	43.1559	60.4703	60.6489	59.5043	71.1985	71.7611	62.0773	73.5126	73.2225	62.5214	73.8217	74.5939	65.7528	75.8609	75.8609	75.8609	75.8609	75.8609	75.8609	75.8609	75.8609	75.8609	
	cameraman	64.0208	71.9292	70.9393	53.0224	54.7578	54.0572	51.861	63.5766	64.213	59.504	71.9698	72.3839	59.1295	67.4435	70.517	60.3015	71.4455	70.5417	70.5417	67.9183	67.9183	67.9183	67.9183	67.9183	67.9183	
Fitness	Pepper	67.1652	71.9344	74.7074	42.1517	57.0011	57.4222	56.4828	67.6826	68.8898	71.1132	78.3264	76.1797	66.9241	74.7322	72.2909	73.0964	80.2535	80.2535	80.2535	76.9183	76.9183	76.9183	76.9183	76.9183	76.9183	
	Gold-hill	66.2242	75.9083	83.8307	40.7799	57.2612	56.8375	56.5584	68.5739	68.8122	71.9043	78.0769	78.0769	65.9821	74.247	73.928	77.9993	80.0453	80.0453	80.0453	79.752	79.752	79.752	79.752	79.752	79.752	
	Lena	46.315	47.8418	49.6905	29.222	40.2322	41.0864	40.09085	43.9634	45.2577	52.804	51.8975	54.09975	46.62135	50.1287	50.53125	50.53125	54.0755	54.0755	54.0755	54.0755	54.0755	54.0755	54.0755	54.0755	54.0755	54.0755
	Iris	44.7973	47.8854	48.4612	28.2754	38.9624	39.5863	39.10205	44.6241	45.8381	50.8333	49.1014	52.36605	44.84245	47.90895	49.03255	49.03255	54.083325	54.083325	54.083325	54.083325	54.083325	54.083325	54.083325	54.083325	54.083325	54.083325
	Baboon	44.5547	47.303	47.38365	28.7269	39.3344	39.63515	39.20385	43.3658	45.5426	40.73815	46.39525	47.44435	41.05045	45.73935	47.21575	47.21575	42.43175	42.43175	47.651	47.651	48.2893	48.2893	48.2893	48.2893	48.2893	48.2893
	cameraman	41.72855	44.26045	45.7025	34.7027	35.83394	36.0139	34.97995	41.1495	41.5345	38.9865	45.1729	45.5437	39.0485	42.1131	45.7933	39.5886	44.71665	45.87885	45.87885	45.87885	45.87885	45.87885	45.87885	45.87885	45.87885	45.87885
	Pepper	43.98925	46.61585	48.0544	28.5805	37.65405	38.7756	37.7785	43.0815	44.2449	46.4195	48.51975	49.0198	44.0037	48.2485	46.90755	46.90755	47.5195	47.5195	47.5195	47.5195	47.5195	47.5195	47.5195	47.5195	47.5195	47.5195
	Gold-hill	43.4686	47.438	52.2914	27.7516	32.7756	38.2683	37.5276	44.5276	44.6221	46.5486	49.02645	49.76955	43.29605	46.9879	47.39865	47.39865	50.60798	50.60798	49.73855	49.73855	49.73855	49.73855	49.73855	49.73855	49.73855	49.73855
	Lena	18.9459	19.6558	21.3508	12.0113	14.8524	17.2303	19.2801	18.4385	19.3376	23.445	21.3188	23.4532	18.8121	19.976	21.281	21.281	23.4681	23.4681	23.4681	23.4681	23.4681	23.4681	23.4681	23.4681	23.4681	23.4681
	Iris	18.6373	18.5217	20.9292	11.7622	13.8933	17.2594	15.9219	17.2216	20.1501	22.3637	18.8071	22.4481	18.4854	20.7572	20.8634	20.8634	23.1675	23.1675	17.0227	17.0227	17.0227	17.0227	17.0227	17.0227	17.0227	17.0227
SDME	Baboon	18.0582	18.7665	19.2262	11.6328	16.1899	16.6042	15.5807	18.3402	18.4071	19.4018	19.7951	20.0542	17.7648	18.6954	18.7783	18.7783	20.6288	20.6288	18.0375	18.0375	15.6883	15.6883	15.6883	15.6883	15.6883	15.6883
	cameraman	17.904	18.076	18.9246	15.9936	15.7463	17.9887	15.441	17.2092	17.8118	18.3418	17.5189	18.5827	17.5104	18.005	18.4248	18.4248	16.6719	16.6719	16.6719	16.6719	16.6719	16.6719	16.6719	16.6719	16.6719	16.6719
	Pepper	18.3975	17.9557	20.2275	12.1033	15.9618	16.4387	16.4965	18.2506	19.0042	17.9064	17.1527	20.9959	18.263	18.1673	19.5293	19.5293	21.4939	21.4939	21.4939	21.4939	21.4939	21.4939	21.4939	21.4939	21.4939	21.4939
	Gold-hill	17.9958	19.5184	21.5057	11.9087	16.4969	19.2823	15.5301	18.2145	18.7018	20.2254	19.5098	20.4566	17.8759	18.5209	19.0929	19.0929	21.031	21.031	19.8772	19.8772	21.031	21.031	21.031	21.031	21.031	21.031
	Lena	58.1343	69.5449	71.3509	34.6617	51.9532	50.7599	61.4921	61.7089	62.3205	81.5382	85.2257	84.2035	58.8635	71.5795	71.8827	71.8827	84.0724	84.0724	84.0724	84.0724	84.0724	84.0724	84.0724	84.0724	84.0724	84.0724
	Iris	55.563	66.1003	68.2369	32.6693	50.3914	50.6074	47.087	61.7903	61.1702	72.2909	79.8829	56.4369	68.7428	69.5557	69.5557	82.7584	82.7584	82.7584	82.7584	82.7584	82.7584	82.7584	82.7584	82.7584	82.7584	
	Baboon	58.1206	58.1351	67.7208	35.8816	48.8136	55.6296	43.1841	52.4805	53.0545	59.5056	60.6602	47.3273	49.05225	51.1855	51.1855	44.775	44.775	44.775	44.775	44.775	44.775	44.775	44.775	44.775	44.775</	

Table 3. (Continued).

$\sigma_n = 70$	PSNR	Images	Average filter			Gaussian filter			Median filter			BPSO-W			BPSO-A			BProposed		
			BD	BDPSO	Proposed	BD	BDPSO	Proposed	BD	BDPSO	Proposed	BD	BDPSO	Proposed	BD	BDPSO	Proposed	BD	BDPSO	Proposed
SDME	Lena	16.4411	16.8539	19.72	9.3853	15.2384	15.4506	12.7837	17.8544	18.077	21.7148	19.7812	21.7171	15.9972	19.4478	19.8307	21.8132	20.6358	22.2203	
	Iris	16.1918	19.1389	19.699	10.5299	14.6354	15.2912	15.5247	17.784	17.7864	21.2771	20.4862	21.4946	15.7175	17.4684	19.6487	21.2346	21.2365	22.003	
	Baboon	15.9309	17.0224	18.6952	10.4124	12.9731	14.6574	13.2295	16.3325	16.8332	19.3312	17.1179	19.6729	15.433	17.4105	18.1905	19.6812	19.0446	20.0048	
	cameraman	15.8437	16.8817	17.6482	13.098	14.3102	14.6229	14.3471	16.0319	16.6109	17.7262	16.2522	18.2151	15.4857	17.5337	17.8723	18.5251	18.2765	18.6694	
	Pepper	16.1271	17.8345	19.1898	10.7872	15.0903	15.4521	13.4039	16.9392	17.3464	19.3107	19.0288	20.0451	15.7658	18.4376	19.1709	20.1084	19.453	20.1544	
	Gold-hill	15.8648	18.3152	18.4809	10.6907	14.6535	15.4667	13.1953	14.6671	16.8445	19.6963	18.851	19.9436	15.4978	18.413	19.5149	19.8544	18.87	20.2254	
	Lena	51.4195	66.0426	66.5549	27.9681	46.4404	46.6871	39.4765	56.6545	57.0127	71.0009	77.6714	77.1609	51.4729	66.8405	66.5557	71.4287	78.2657	78.7091	
	Iris	48.9411	63.8069	64.7857	29.2977	44.93	45.3433	48.8676	55.0028	55.7576	66.7818	74.2571	74.8943	49.1845	63.9871	64.1038	66.5817	75.0634	75.0778	
	Baboon	51.7704	66.88275	67.3518	31.0319	41.4127	47.4233	42.5302	57.323	58.5011	68.1288	75.7286	76.4951	51.8414	66.3625	67.2094	70.3962	77.7742	78.1178	
	cameraman	49.307	65.009	65.1871	39.1878	44.2218	44.9334	44.6576	50.8648	51.734	59.5909	70.9897	70.3698	49.3	64.5937	64.5322	68.4509	74.1355	75.1653	
	Pepper	50.4206	64.9378	65.071	30.1643	44.6591	45.7236	39.8018	54.7869	54.7236	63.0421	73.5899	72.6737	50.2781	65.7023	65.988	70.0308	76.4028	76.7657	
	Gold-hill	48.8787	63.7275	64.7038	29.0884	43.2715	44.5326	38.2569	49.7402	54.5141	68.0532	74.9603	75.9584	49.094	64.1659	64.5149	69.3344	75.3716	77.0068	
Fitness	Lena	33.9303	41.44825	43.13745	18.6767	30.8394	31.06885	26.1301	37.25445	37.54485	46.35785	48.7763	49.4339	33.73505	43.14115	43.2432	46.62095	49.45075	50.4647	
	Iris	32.56645	41.4729	42.24235	19.19138	29.7827	30.31725	32.19615	36.3934	36.7722	44.02945	47.37165	48.19445	32.451	40.72775	41.87625	43.90815	48.14995	48.5404	
	Baboon	33.85065	41.92495	43.0235	20.77215	12.9731	31.04035	27.87985	36.82775	37.66715	43.73	46.42325	48.084	33.6372	41.8865	42.69995	45.0387	48.4094	49.0613	
	cameraman	32.57535	40.94535	41.41765	26.1429	29.266	29.77815	29.50235	33.44835	34.17245	38.6555	43.62095	44.29245	33.39285	41.0937	41.20225	43.4388	46.2026	46.91735	
	Pepper	33.27385	41.38615	42.1304	20.47575	29.8747	30.38785	26.60285	35.86305	36.035	41.1764	46.30935	46.3594	33.02195	42.06995	42.58445	45.0696	47.9279	48.46005	
	Gold-hill	32.37175	41.02135	41.59235	28.9625	29.9965	25.7261	32.20365	35.6793	43.87475	46.90565	47.951	32.2959	41.28945	42.0149	44.5944	47.1208	48.6161		

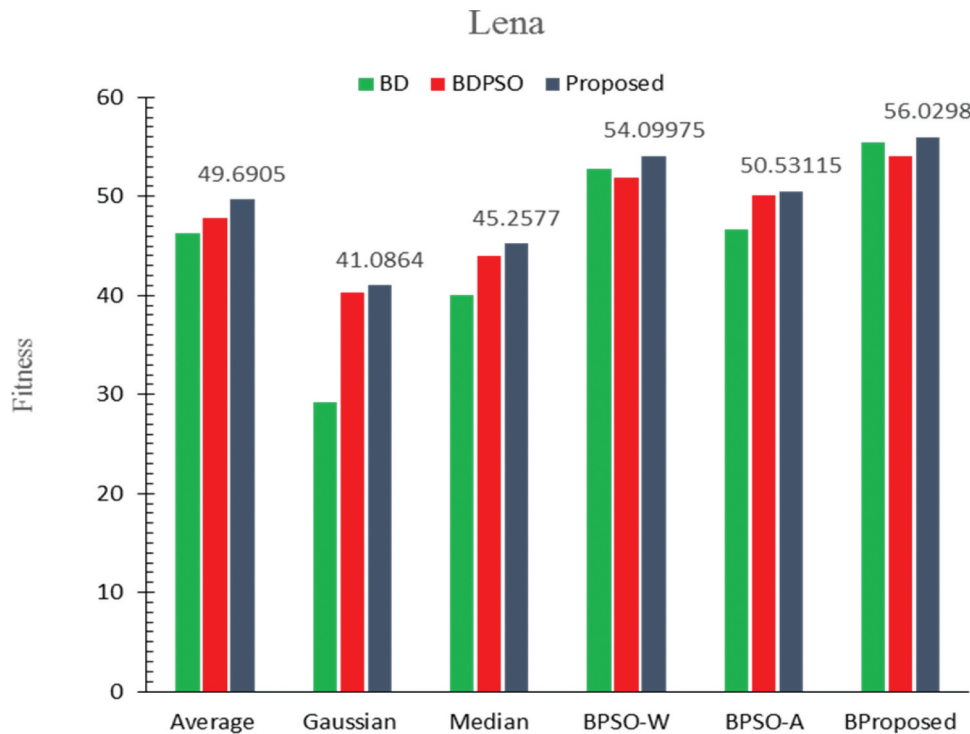


Figure 8. PSNR value of the proposed restoration method, BD and BDPSO techniques.

(σ_d, σ_r) of the bilateral filter were optimized for minimizing the MSE as the objective function. Therefore, the SSIM value and the PSNR value increased in the proposed filter.

As the results in Table 2 and Figure 6 show, the proposed filter and the PSO-based filters (BPSO-W, BPSO-A) have almost similar results in the SAP noise reduction and have better performance than the average and Gaussian filters but have poorer performance than the median filter. Therefore, it is concluded that the proposed filter is not suitable for SAP noise reduction.

After image noise reduction, the restoration phase was done. R-L algorithm performed the restoration process on the noise-free images. The PSF of the R-L algorithm was optimized by the WOA algorithm and was compared with the BD and BDPSO methods. The PSNR and SDME values were evaluated to compute the performance of the restored image. The fitness function of the proposed restoration method consists of two objective functions, PSNR and SDME, which are automatically calculated by the algorithm. For the BDPSO method, only SDME is automatically calculated by the algorithm, and for the BD method, all of the measures are calculated manually and the results are shown in Table 3. For instance, Figures 8–10 show the PSNR,

SDME, and fitness values of the proposed restoration method compared to the BD and BDPSO techniques on Lena's image for $\sigma_n = 30$. Figure 11 shows the practical restoration results of the proposed method, the BD, and the BDPSO techniques on different noiseless images. In Figure 11, c_1, d_1, e_1, f_1, g_1 , and h_1 represent the images restored by the BD technique on the images obtained from the averages, Gaussian, median, BPSO-W, BPSO-A, and the BProposed filters, respectively, and c_2, d_2, e_2, f_2, g_2 , and h_2 represent the images restored by the BDPSO technique on the images obtained from the average, Gaussian, median, BPSO-W, BPSO-A, and the BProposed filters, respectively and c_3, d_3, e_3, f_3, g_3 , and h_3 represent the images restored by the proposed technique on the images obtained from the average, Gaussian, median, BPSO-W, BPSO-A, and the BProposed filters, respectively.

As shown in Table 3 and Figures 8–10, the proposed method attained higher PSNR and fitness values than the BD and BDPSO techniques for all trial images. The high value of the fitness function showed better image restoration. Although in most images, the SDME value of the proposed method is higher, in some images, this value is higher for the BDPSO method, and the reason is that in the BDPSO method, only the SDME value is maximized. No attention is paid to the PSNR values of

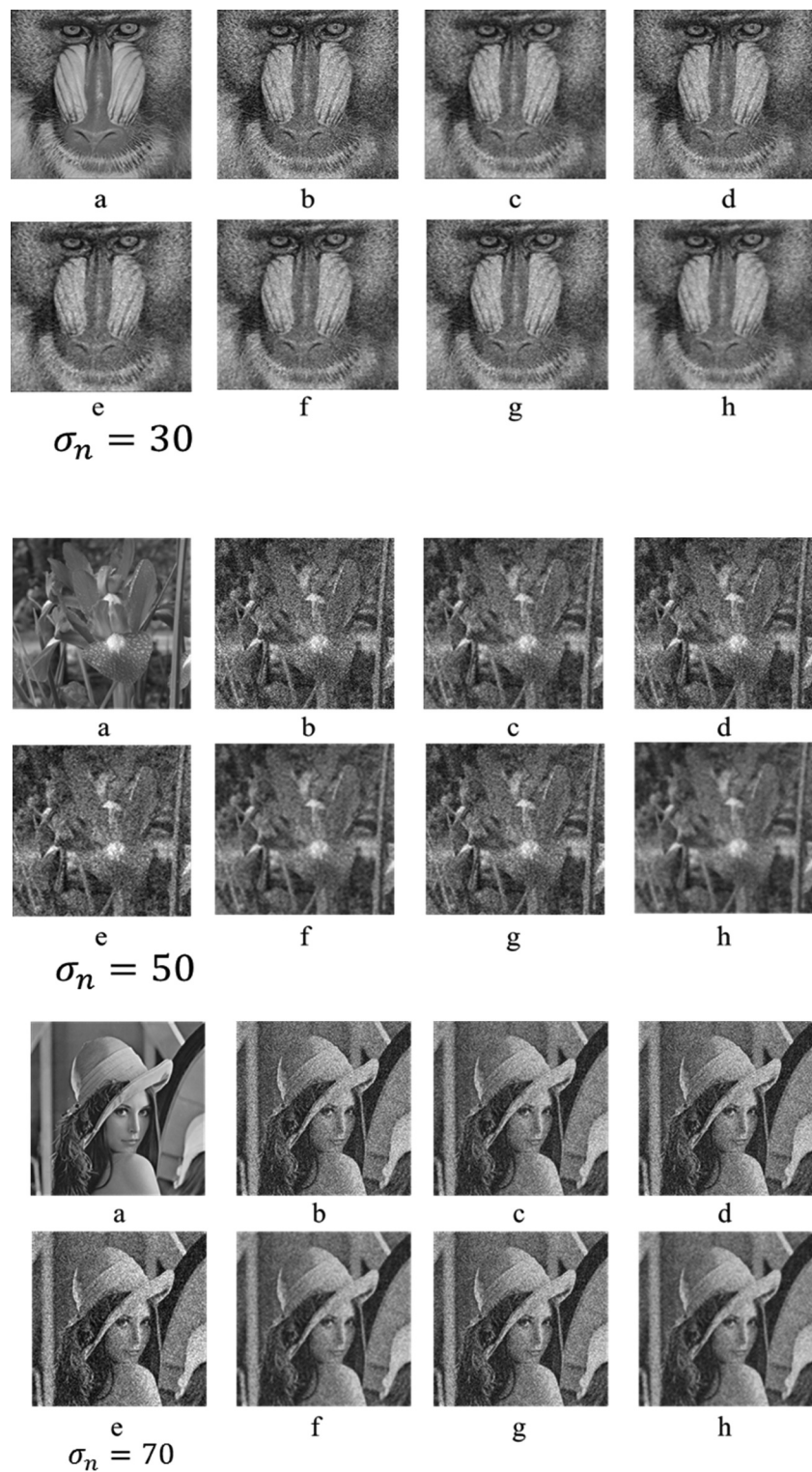


Figure 9. SDME value of the proposed restoration method, BD and BDPSO techniques.

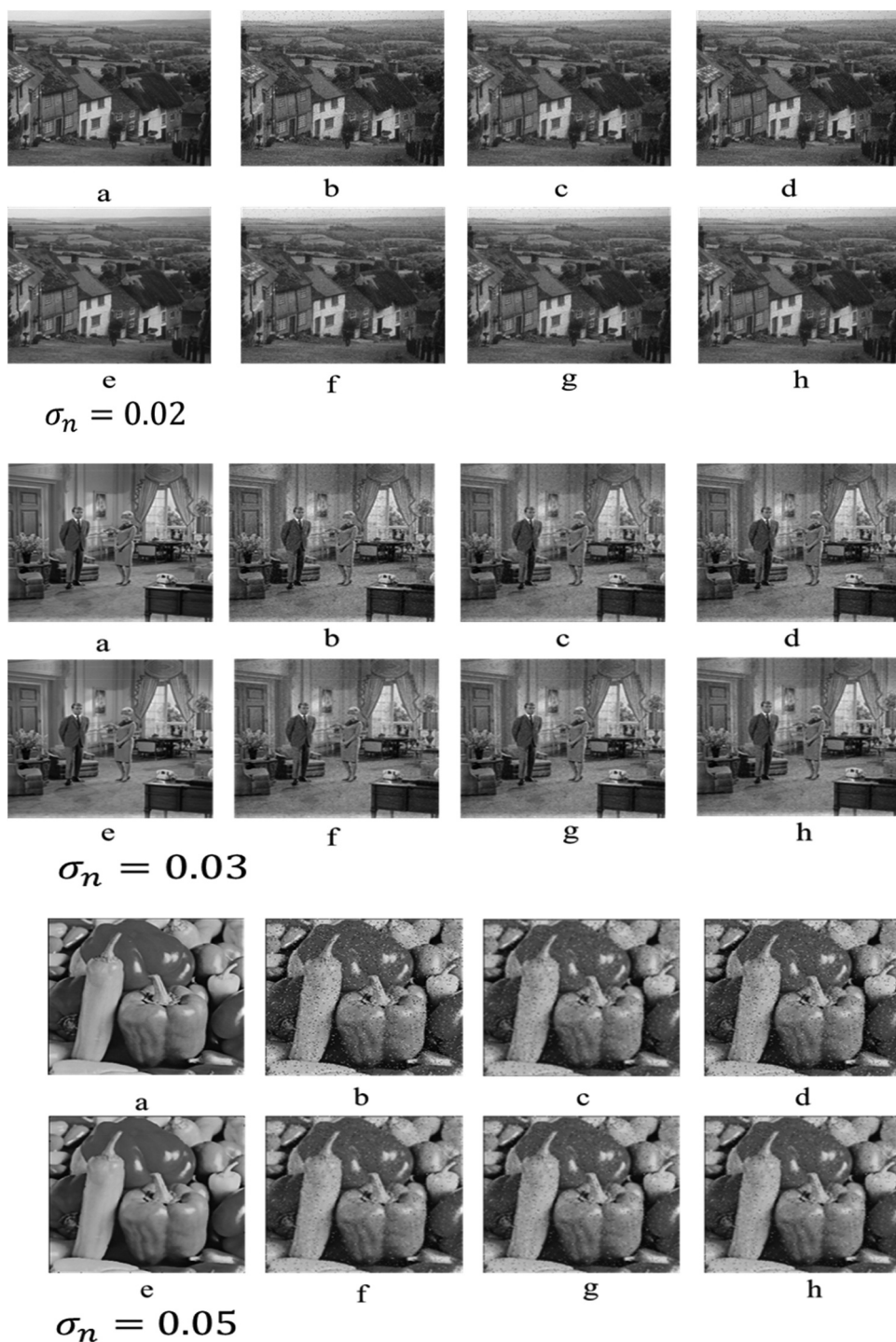


Figure 10. The fitness value of the proposed restoration method, BD and BDPSO techniques.

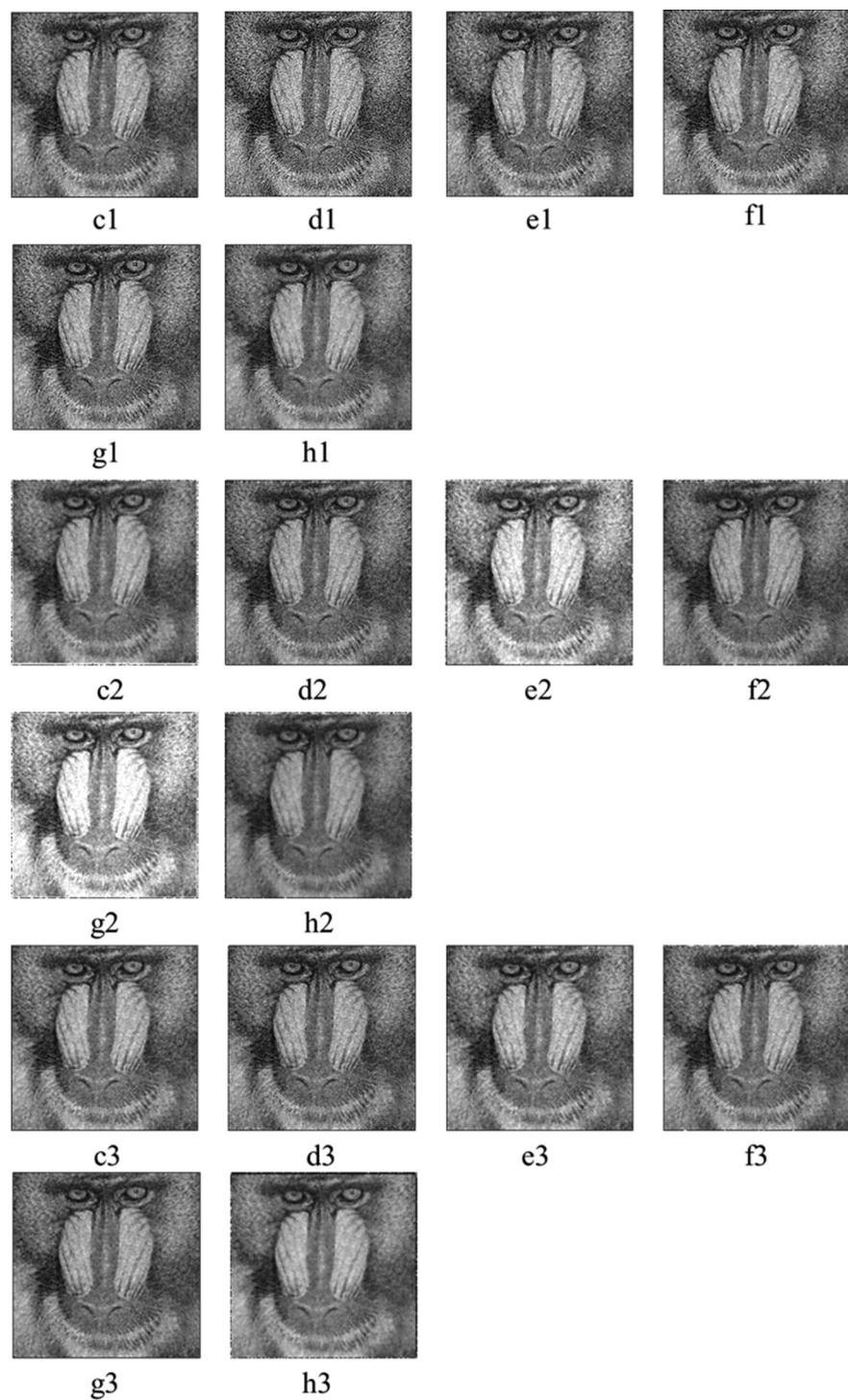
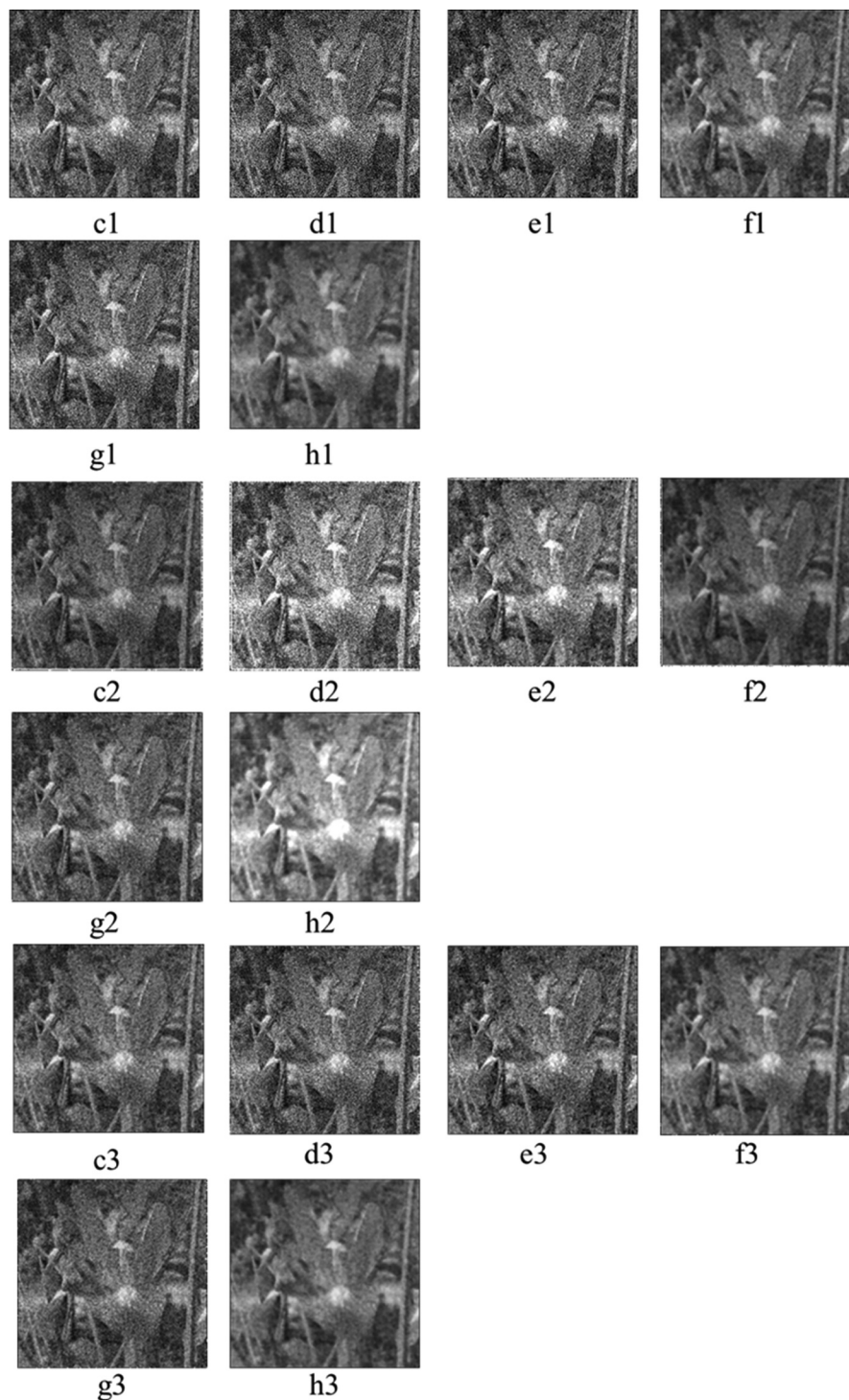


Figure 11. Images resulting from image restoration techniques.



$$\sigma_n = 50$$

Figure 11. Continued.

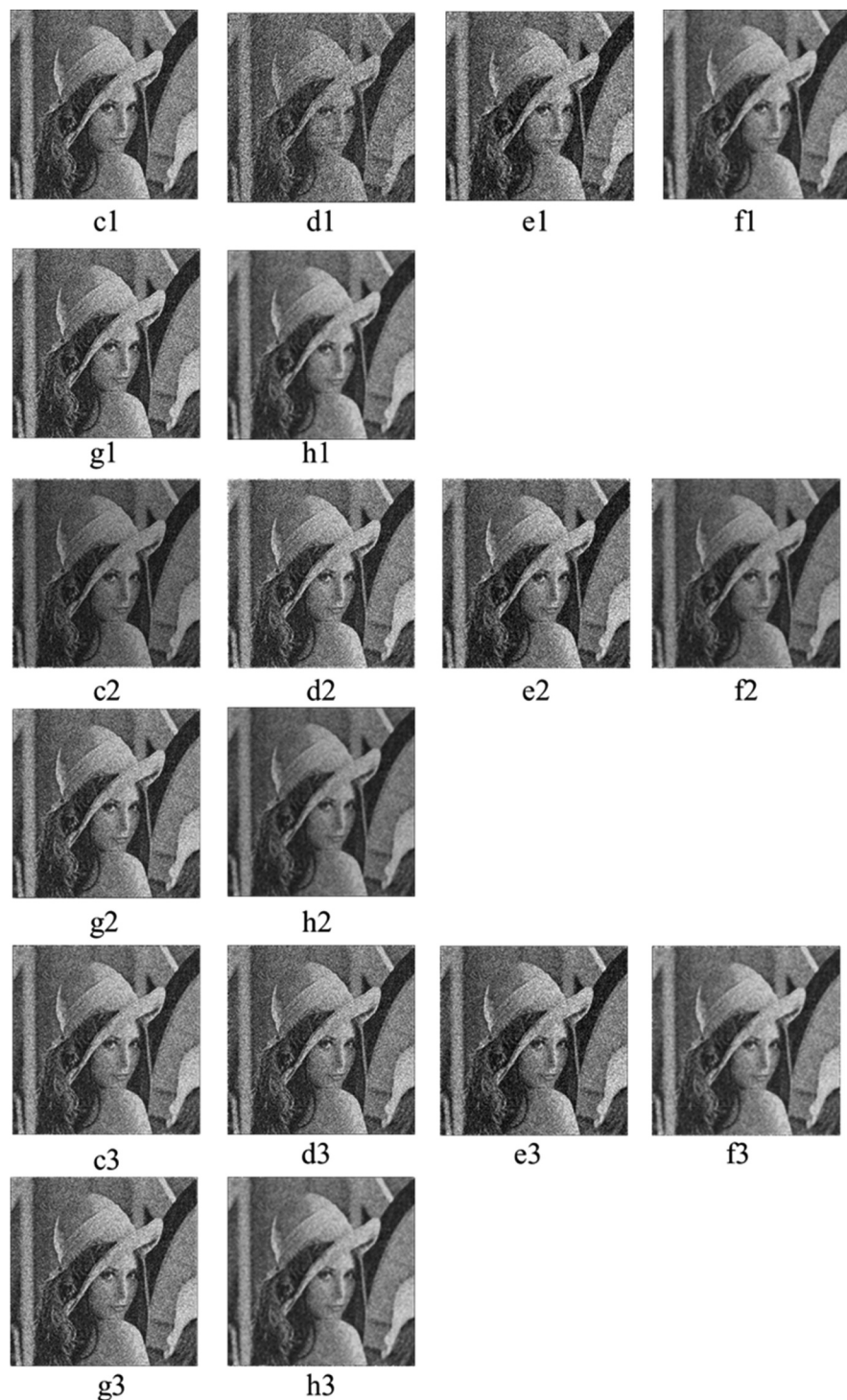


Figure 11. Continued.

the images. In fact, in the proposed method, as the SDME increases, the PSNR of the output image also increases. This makes the proposed method superior to other methods.

6. Conclusion

The filter-based denoising techniques can effectively reduce the noise but cannot preserve the image quality and information; therefore, metaheuristic algorithms have been used. The meta-heuristic algorithms play an important role in replacing human inspections and interpreting processed images. This paper used the WOA algorithm in the bilateral filter and the R-L algorithm for denoising and restoring the grayscale images, respectively. The intensity domain parameter, spatial domain parameter, and radius parameter of the bilateral filter were optimized by considering the weighted sum of the PSNR and SSIM values as a fitness function and using the WOA algorithm. The noise-free image was achieved and compared with existing noise removal filters such as average, Gaussian, median, BPSO-W, and BPSO-A. The noise-free image seemed to have a few blurring effects, so the noiseless image was restored by optimizing the PSF of the R-L algorithm and considering the weighted sum of the PSNR and SDME values as a fitness function via the WOA algorithm and was compared with BD, and BDPSO. The proposed noise removal technique results showed that it had better performance for all levels of the Gaussian noise compared to the classical and PSO-based techniques.

The superiority of the proposed method over the PSO-based methods is that the intensity domain parameter, spatial domain parameter, and the radius parameter of the bilateral filter were optimized simultaneously, and, in addition to maximizing the SSIM value, the PSNR value was also maximized. However, the proposed method performs similarly to the PSO-based methods in SAP noise reduction. Like them, it performs better than the average and Gaussian filters but poorly compared to the median filter. Therefore, the median filter performance was better than all methods in SAP noise removal. The results also indicated that the proposed method obtained better restoration performance. The PSNR value of the proposed method is higher in all filtered images than in the other methods, and the SDME value is higher in most images. This value is sometimes higher for the PSO-based method simply due to the maximization of this criterion in that algorithm, which reduces the PSNR value of the images. One of the advantages of the proposed noise reduction filter is

the preservation of image information after significant noise reduction and its simple design. Disadvantages of the proposed methods are the unavailability of the noiseless original image, the lack of certain limits for the parameters, and the use of the weighted sum method to solve a multi-objective problem that causes some answers to be lost.

Further investigations should be done using the Cauchy distribution to make a mask for noise removal or filter design using the MOPSO algorithm to solve the multi-objective problems. For future work, adaptive meta-heuristic algorithms can also be used to increase convergence speed. The noiseless images can also be restored by the Bilal et al. (Bilal et al., 2016; OIRIPSA) method, which has been claimed to give better results than the Richardson Lucy technique. The proposed technique in the current paper has been fundamental and can be applied to different image applications such as medical, satellite, colored images, etc.

Notes

1. Peak signal to noise ratio.
2. Structural similarity index measure.
3. Second derivative like measure enhancement.
4. Nondeterministic polynomial time.
5. Particle swarm optimization.
6. Point spread function.
7. Wavelet packet.
8. Bayesian least-squares Gaussian scale mixture.
9. Support vector machine classification.
10. Higher-order singular value decomposition.
11. Nearest neighbors.
12. Statistical nearest neighbors.
13. Adaptive weighted mean filter.
14. Fuzzy filter.
15. Bayesian non-local means filter.
16. Multi-objective PSO Association Rule Mining.
17. Adaptive genetic algorithm.
18. Generalized Cauchy.
19. Multi-objective particle swarm optimization.
20. Adaptive particle swarm optimization.
21. Richardson Lucy.

Disclosure statement

No potential conflict of interest was reported by the author(s).

Funding

The authors received no direct funding for this research.

ORCID

Farzin Modarres Khiyabani  <http://orcid.org/0000-0002-7688-2535>

References

- Asokan, A., & Anitha, J. (2020). Adaptive cuckoo search based optimal bilateral filtering for denoising of satellite images. *ISA transactions*, 100, 308–321. <https://doi.org/10.1016/j.isatra.2019.11.008>
- Bilal, M., Wyne, M. F., & Jaffar, M. A. Image restoration by multivariate-stochastic optimization using improved particle swarm algorithm. In *Evolutionary Computation (CEC), 2016 IEEE Congress on*, 2016, pp. 2596–2603. <https://doi.org/10.1109/cec.2016.7744113>
- Chen, B., Cai, J.-L., Chen, W.-S., & Li, Y. (2012). A multiplicative noise removal approach based on partial differential equation model. *Mathematical Problems in Engineering*, 2012, 1–14. <https://doi.org/10.1155/2012/242043>
- Cho, T. S., Zitnick, C. L., Joshi, N., Kang, S. B., Szeliski, R., & Freeman, W. T. (2012). Image restoration by matching gradient distributions. *IEEE Transactions on Pattern Analysis and Machine Intelligence*, 34(4), 683–694. <https://doi.org/10.1109/tpami.2011.166>
- Conte, F., Germani, A., & Iannello, G. (2013). A Kalman filter approach for denoising and deblurring 3-d microscopy images. *IEEE Transactions on Image Processing*, 22(12), 5306–5321. <https://doi.org/10.1109/cdc.2013.6761107>
- Dash, R., & Majhi, B. (2014). Motion blur parameters estimation for image restoration. *Optik-International Journal for Light and Electron Optics*, 125(5), 1634–1640. <https://doi.org/10.1016/j.ijleo.2013.09.026>
- Dou, L., Xu, D., Chen, H., & Liu, Y. Image de-noising based on mathematical morphology and multi-objective particle swarm optimization. In *Ninth International Conference on Digital Image Processing (ICDIP 2017)*, 2017, p. 104202I. <https://doi.org/10.1117/12.2281560>
- Eberhart, R., & Kennedy, J. (1995). A new optimizer using particle swarm theory. In *Micro Machine and Human Science, 1995. MHS'95., Proceedings of the Sixth International Symposium on*, pp. 39–43. <https://doi.org/10.1109/mhs.1995.494215>
- Fathi, A., & Naghsh-Nilchi, A. R. (2012). Efficient image denoising method based on a new adaptive wavelet packet thresholding function. *IEEE Transactions on Image Processing*, 21(9), 3981–3990. <https://doi.org/10.1109/tip.2012.2200491>
- Fish, D., Brinicombe, A., Pike, E., & Walker, J. (1995). Blind deconvolution by means of the Richardson-Lucy algorithm. *JOSA A*, 12(1), 58–65. <https://doi.org/10.1364/josaa.12.000058>
- Frosio, I., & Kautz, J. (2018). Statistical nearest neighbors for image denoising. *IEEE Transactions on Image Processing*, 28(2), 723–738. <https://doi.org/10.1109/tip.2018.2869685>
- Fu, H. X., Wang, Y. C., & Su, X. (2014). Restoration of motion blurred image based on PSO combine wiener filter in ship imaging system. *Advanced Materials Research*, 1006-1007, 739–742. <https://doi.org/10.4028/www.scientific.net/AMR.1006-1007.739>
- Goyal, B., Dogra, A., Agrawal, S., Sohi, B., & Sharma, A. (2020). Image denoising review: From classical to state-of-the-art approaches. *Information Fusion*, 55, 220–244. <https://doi.org/10.1016/j.inffus.2019.09.003>
- Gulat, N., & Kaushik, A. (2012). Remote sensing image restoration using various techniques: A review. *International Journal of Scientific & Engineering Research*, 3. <https://doi.org/10.1109/igarss47720.2021.9555039>
- Hassani, H., Mahmoudvand, R., & Yarmohammadi, M. (2010). Filtering and denoising in linear regression analysis. *Fluctuation and Noise Letters*, 9(4), 343–358. <https://doi.org/10.1142/s0219477510000289>
- Karami, A., & Tafakori, L. (2017). Image denoising using generalised Cauchy filter. *IET Image Processing*, 11(9), 767–776. <https://doi.org/10.1049/iet-ipr.2016.0554>
- Karnati, V., Uliyar, M., & Dey, S. Fast non-local algorithm for image denoising. In *2009 16th IEEE International Conference on Image Processing (ICIP)*, 2009, pp. 3873–3876. <https://doi.org/10.1109/icip.2009.5414044>
- Khalaf, T. Z., Çağlar, H., Çağlar, A., & Hanoon, A. N. (2020). Particle swarm optimization based approach for estimation of costs and duration of construction projects. *Civil Engineering Journal*, 6(2), 384–401. <https://doi.org/10.28991/cej-2020-03091478>
- Kumar, N., Shukla, H., & Tripathi, R. (2017). Image restoration in noisy free images using fuzzy based median filtering and adaptive particle swarm optimization-Richardson-Lucy algorithm. *International Journal of Intelligent Engineering and Systems*, 10(4), 50–59. <https://doi.org/10.2266/ijies2017.0831.06>
- Lateef, H. H., & Burhan, A. M. (2019). Time-cost-quality trade-off model for optimal pile type selection using discrete particle swarm optimization algorithm. *Civil Engineering Journal*, 5(11), 2461–2471. <https://doi.org/10.28991/cej-2019-03091424>
- Lee, C., Lee, C., & Kim, C.-S. (2012). An MMSE approach to nonlocal image denoising: Theory and practical implementation. *Journal of Visual Communication and Image Representation*, 23(3), 476–490. <https://doi.org/10.1016/j.jvcir.2012.01.007>
- Lin, T.-C. (2011). Decision-based fuzzy image restoration for noise reduction based on evidence theory. *Expert Systems with Applications*, 38(7), 8303–8310. <https://doi.org/10.1016/j.eswa.2011.01.016>
- Lv, X.-G., Song, Y.-Z., Wang, S.-X., & Le, J. (2013). Image restoration with a high-order total variation minimization method. *Applied Mathematical Modelling*, 37(16–17), 8210–8224. <https://doi.org/10.1016/j.apm.2013.03.028>
- Mamta, G. R., & Dutta, M. (2018). PSO based blind deconvolution technique of image restoration using cepstrum domain of motion blur. In Mamta, G. R. & Dutta, M. (Eds.) *Computational vision and bio inspired computing* (pp. 947–958). Springer. https://doi.org/10.1007/978-3-319-71767-8_81
- Mirjalili, S., & Lewis, A. (2016). The whale optimization algorithm. *Advances in Engineering Software*, 95, 51–67. <https://doi.org/10.1016/j.advengsoft.2016.01.008>
- Moreno, J., Jaime, B., & Saucedo, S. (2013). Towards no-reference of peak signal to noise ratio. *Editorial Preface*, 4. <https://doi.org/10.14569/ijacs.2013.040119>
- Pan, H., Wen, Y.-W., & Zhu, H.-M. (2019). A regularization parameter selection model for total variation based image noise removal. *Applied Mathematical Modelling*, 68, 353–367. <https://doi.org/10.1016/j.apm.2018.11.032>
- Rajwade, A., Rangarajan, A., & Banerjee, A. (2013). Image denoising using the higher order singular value decomposition. *IEEE Transactions on Pattern Analysis and Machine Intelligence*, 35(11), 2678–2691. <https://doi.org/10.1109/tpami.2013.50>

- and Machine Intelligence*, 35(4), 849–862. <https://doi.org/10.1109/tpami.2012.140>
- Roy, A., Singha, J., Devi, S. S., & Laskar, R. H. (2016). Impulse noise removal using SVM classification based fuzzy filter from gray scale images. *Signal Processing*, 128, 262–273. <https://doi.org/10.1016/j.sigpro.2016.04.007>
- Sakthidasan, K., & Nagappan, N. V. (2016). Noise free image restoration using hybrid filter with adaptive genetic algorithm. *Computers & Electrical Engineering*, 54, 382–392. <https://doi.org/10.1016/j.compeleceng.2015.12.011>
- Saljoughi, A. S., Mehrvarz, M., & Mirvaziri, H. (2017). Attacks and intrusion detection in cloud computing using neural networks and particle swarm optimization algorithms. *Emerging Science Journal*, 1, 179–191. <https://doi.org/10.28991/ijse-01120>
- Sankaran, K. S., Bhuvaneshwari, S., & Nagarajan, V. A new edge preserved technique using iterative median filter. In *Communications and Signal Processing (ICCSP), 2014 International Conference on*, 2014, pp. 1750–1754. <https://doi.org/10.1109/iccsp.2014.6950146>
- Satpathy, S., Panda, S., Nagwanshi, K., & Ardin, C. (2010). Image restoration in non-linear filtering domain using MDB approach. *International Journal of Signal Processing*, 6, 1. <https://doi.org/10.1109/rteict42901.2018.9012420>
- Tirer, T., & Giryen, R. (2018). Image restoration by iterative denoising and backward projections. *IEEE Transactions on Image Processing*, 28(3), 1220–1234. <https://doi.org/10.1109/tip.2018.2875569>
- Tomasi, C., & Manduchi, R. (1998). Bilateral filtering for gray and color images. *Iccv*, 2. <https://doi.org/10.1109/iccv.1998.710815>
- VaeziNejad, S., Marandi, S., & Salajegheh, E. (2019). A hybrid of artificial neural networks and particle swarm optimization algorithm for inverse modeling of leakage in earth dams. *Civil Engineering Journal*, 5(9), 2041–2057. <https://doi.org/10.28991/cej-2019-03091392>
- Varzaneh, H. H., Neysiani, B. S., Ziafat, H., & Soltani, N. (2018). Recommendation systems based on association rule mining for a target object by evolutionary algorithms. *Emerging Science Journal*, 2(2), 100–107. <https://doi.org/10.28991/esj-2018-01133>
- Wang, Z., Bovik, A. C., Sheikh, H. R., & Simoncelli, E. P. (2004). Image quality assessment: From error visibility to structural similarity. *IEEE Transactions on Image Processing*, 13(4), 600–612. <https://doi.org/10.1109/tip.2003.819861>
- Wang, Y., Wang, J., song, X., & Han, L. (2016). An efficient adaptive fuzzy switching weighted mean filter for salt-and-pepper noise removal. *IEEE Signal Processing Letters*, 23 (11), 1582–1586. <https://doi.org/10.1109/lsp.2016.2607785>
- Wang, C., Xue, B., & Shang, L. PSO-based parameters selection for the bilateral filter in image denoising. In *Proceedings of the Genetic and Evolutionary Computation Conference*, 2017, pp. 51–58. <https://doi.org/10.1145/3071178.3071231>
- Wang, X.-Y., Yang, H.-Y., & Fu, Z.-K. (2013). Edge structure preserving image denoising using OAGSM/NC statistical model. *Digital Signal Processing*, 23(1), 200–212. <https://doi.org/10.1016/j.dsp.2012.09.002>
- Wiener, N. (1975). Extrapolation, interpolation, and smoothing of stationary time series. <https://doi.org/10.7551/mitpress/2946.001.0001>
- Yang, X.-S., & Deb, S. (2009). Cuckoo search via Lévy flights. *Nature & Biologically Inspired Computing*, 210–214. 2009. *NabIC 2009. World Congress on*. <https://doi.org/10.1109/nabic.2009.5393690>
- Yang, L., Parton, R., Ball, G., Qiu, Z., Greenaway, A. H., Davis, I., & Lu, W. (2010). An adaptive non-local means filter for denoising live-cell images and improving particle detection. *Journal of Structural Biology*, 172(3), 233–243. <https://doi.org/10.1016/j.jsb.2010.06.019>
- Ye, Z. Y. (2013). Image restoration based on improved PSO algorithm. *Advanced Materials Research*, 2249–2252. <https://doi.org/10.4028/www.scientific.net/amr.605–607.2249>
- Zhang, Y., Duijster, A., & Scheunders, P. (2012). A Bayesian restoration approach for hyperspectral images. *IEEE Transactions on Geoscience and Remote Sensing*, 50(9), 3453–3462. <https://doi.org/10.1109/tgrs.2012.2184122>
- Zhang, H., He, W., Zhang, L., Shen, H., & Yuan, Q. (2014). Hyperspectral image restoration using low-rank matrix recovery. *IEEE Transactions on Geoscience and Remote Sensing*, 52(8), 4729–4743. <https://doi.org/10.1109/tgrs.2013.2284280>
- Zhang, P., & Li, F. (2014). A new adaptive weighted mean filter for removing salt-and-pepper noise. *IEEE Signal Processing Letters*, 21(10), 1280–1283. <https://doi.org/10.1109/lsp.2014.2333012>
- Zhang, H., Yang, J., Zhang, Y., & Huang, T. S. (2013). Image and video restorations via nonlocal kernel regression. *IEEE Transactions on Cybernetics*, 43(3), 1035–1046. <https://doi.org/10.1109/tsmc.2012.2222375>
- Zhou, Y., Zang, H., Xu, S., He, H., Lu, J., & Fang, H. (2019). An iterative speckle filtering algorithm for ultrasound images based on Bayesian nonlocal means filter model. *Biomedical Signal Processing and Control*, 48, 104–117. <https://doi.org/10.1016/j.bspc.2018.09.011>